5-2015

Novel Polyurethane Foams Derived from Bio-Based Materials

Nelson Elbers
Pittsburg State University

NOVEL POLYURETHANE FOAMS DERIVED FROM BIO-BASED MATERIALS

A Thesis Submitted to the Graduate School
In Partial Fulfillment of the Requirements
For The Degree of Master of Science

Nelson Elbers

Pittsburg State University

Pittsburg, Kansas

May, 2015

NOVEL POLYURETHANE FOAMS DERIVED FROM BIO-BASED MATERIALS

Nelson Elbers

APPROVED:

Thesis Advisor _____
Dr. Ram Gupta, Chemistry Department

Committee Member _____
Dr. Khamis Siam, Chemistry Department

Committee Member _____
Dr. William Shirley, Chemistry Department

Committee Member _____
Dr. Ivan Javni, Kansas Polymer Research Center

Committee Member _____
Dr. John Franklin, Department of English and Modern Languages

ACKNOWLEDGEMENTS

Special thanks go to Dr. Ram Gupta for his expertise, technical support and advising of the project. Thanks go out also to Dr. Khamis Siam and Dr. William Shirley of the Department of Chemistry at Pittsburg State University, Pittsburg, Kansas, for their service on the thesis committee and their advising during the organization of this thesis. Thanks go out to Dr. Ivan Javni of the Kansas Polymer Research Center, Pittsburg, KS, for his presence on the thesis committee as well as his expertise. Thanks go to Dr. John Franklin of the English Department at Pittsburg State University for his membership on the thesis committee as well as his advising during the composition and editing of this thesis. Special thanks go to Dr. Andrew Myers of the Kansas Polymer Research Center, Pittsburg, Kansas, for allowing the use of the facilities and instruments. His generosity made the completion of all experimental work possible. Special thanks also go to Dr. Petar Dvornic of the Department of Chemistry at Pittsburg State University and Dr. Mihail Ionescu of the Kansas Polymer Research Center for their expertise and guidance during the project.

NOVEL POLYURETHANE FOAMS DERIVED FROM BIO-BASED MATERIALS

An Abstract of the Thesis By
Nelson Elbers

The bio-based materials α-phellandrene and β-caryophyllene were used in this research as starting materials for the synthesis of novel bio-based polyurethane foams. The purpose was to assess the properties of the novel bio-based polyurethane foams and to determine whether they could serve as viable options for the commercial application of thermal insulation of buildings, freezers, pipes and storage tanks. The bio-based polyols using α-phellandrene and β-caryophyllene were synthesized. The polyols were synthesized using a photochemical thiol-ene coupling reaction. The hydroxyl groups were attached to the bio-based materials using different mol ratio of 1-thioglycerol and 2-mercaptoethanol. The synthesized bio-based polyols were used to prepare novel polyurethane foams. The polyurethane foams were synthesized using 100% bio-based polyol and a mixture of polyols having 50% bio-based polyol and 50% Jeffol SG-360. A reference polyurethane foam was also prepared using commercially available polyol (Jeffol SG-360). This particular foam served as the industrial reference to which the properties of all the novel polyurethane foams were compared. The properties of foam which were assessed in this research include: closed cell content, density, mechanical property, glass transition temperature, microstructural analysis, and thermal stability. It was found that the prepared polyurethane foams were comparable in property to the industrial reference foam. These foams proved superior to the industrial reference foam

in the properties of closed cell content, glass transition temperature, and mechanical property. Overall, it was determined based on the assessment of their properties that the novel bio-based polyurethane foams which were synthesized and studied in this work could serve as viable options in industry to be used for the purpose of thermal insulation in areas including, but not limited to, buildings, storage tanks, freezers and pipes.

TABLE OF CONTENTS

LIST OF TABLES

LIST OF FIGURES

CHAPTER I

INTRODUCTION

1.1. Bio-based Polymers

Bio-based polymers have attracted considerable academic as well as industrial interest due to sustainability and environmental concerns. Therefore, the search for sustainable development based on renewable bio-based feedstocks has become a major research area [1, 2]. Biomasses from plant-derived resources are renewable raw materials and are capable of providing a wide variety of starting materials for monomers and polymers [3]. Polyurethanes have been widely studied polymers due to their potential applications in industry, biomedical and academic fields [4]. Polyurethane foams are prepared by reacting diisocyanates with compounds containing two or more hydroxyl groups (polyols).

1.2. Polyurethanes: Properties, Formation and Uses

Polyurethanes are used extensively for a variety of applications within the chemical industry [5-8]. The chemical structure of a polyurethane linkage is shown in

Figure 1.1. In the particular case as seen in Figure 1.1, the polyurethane is linear; however, polyurethanes often form cross-linked and branched networks based on functionality of the starting polyols. Polyurethanes are typically formed through the addition-polymerization reaction of diisocyanates with polyols. The functionality, or number of chemical functional group equivalents, which these starting materials possess, must be at least two in order for polymerization to occur [9]. The addition polymerization reaction which is used to produce polyurethanes proceeds by a mechanism which can be seen in Figure 1.2. Cross-linked networks are often formed in polyurethane structure because the polyol components used for the addition polymerization often have functionality which is greater than two. When bifunctional monomers are used for polymerization reactions, a linear polymer is produced. However, when one monomer unit with a functionality of three or more reacts with a bifunctional monomer, a network polymer is produced due to the presence of branch points in the higher functionality monomer.

There are two primary steps involved in the synthesis of polyurethanes: the first is the formation of a polyol, which can have its functionality of hydroxyl groups equal to two or more and the second step is the reaction of a polyol with a diisocyanate to form a polyurethane. The synthesis of polyols is accomplished commonly by a few main routes [10]. For example, polyols have been made through catalyzed ring-opening of epoxidized soybean oil with methanol [11]. They have also been made from divalent alcohols such as ethylene and propylene glycol and from multivalent alcohols such as sucrose and glycerol.

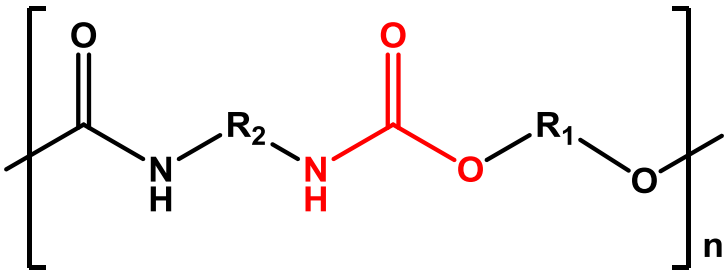

Figure 1.1: Chemical structure of a polyurethane.

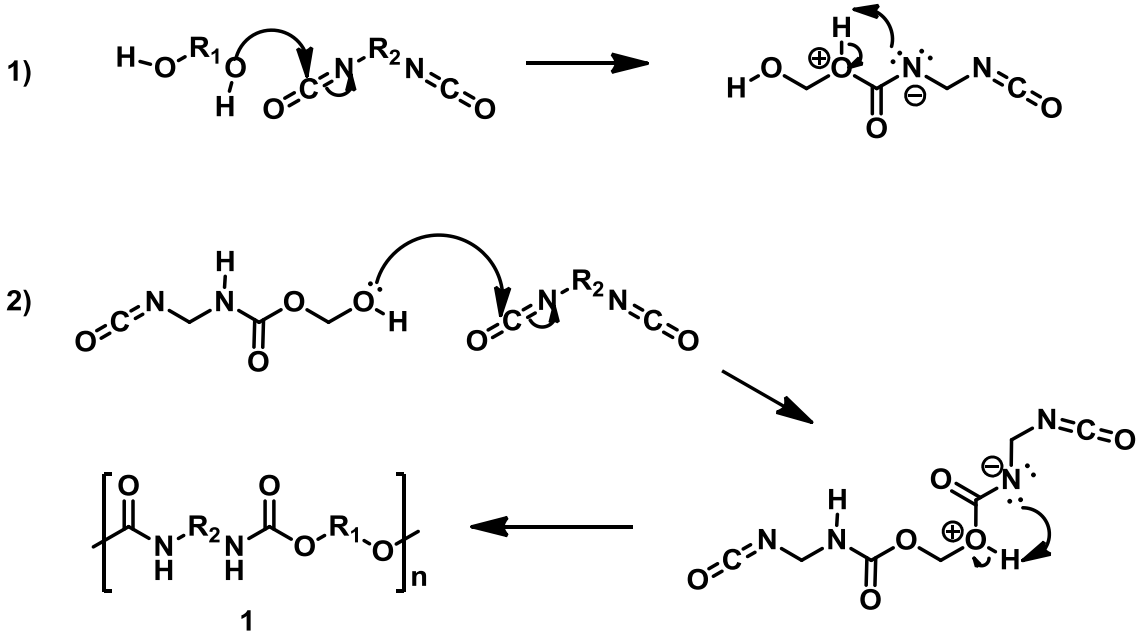

Figure 1.2: General mechanism for the formation of a polyurethane.

Note: Steps 1) and 2) repeat with successive monomeric units until a polymer with a general structure resembling **1** is formed which contains n repeating units

The polyols which are used in the formation of polyurethanes are hydroxy-polyethers primarily. These materials are made by ring-opening polymerization of epoxides such as ethylene and propylene oxide with alcohols which can be divalent or

multivalent. Polyols have also been produced from bio-based material through the thiol-ene reaction of alkene-containing natural products with thiol-containing materials such as 2-mercaptoethanol and 1-thioglycerol [9, 12], methods which will be discussed in more detail later.

There are a variety of important factors which are involved in the preparation of polyurethanes. The diisocyanate molecules used most commonly for preparation of polyurethanes are 2, 4 and 2, 6 isomers of toluenediisocyanate (TDI) and diphenylmethane diisocyanate (MDI) (Figure 1.3). Polyurethanes produced from the aforementioned reaction (Figure 1.2) exhibit properties which are dependent on the functionality of the monomeric materials which are used. The process used to produce polyurethanes involves the use of additional materials to the monomeric polyols and diisocyanate molecules. Generally, a polyurethane foam formulation includes a polyol, isocyanate, surfactant, blowing agent, catalyst, co-catalyst and in some cases, a cross-linker. Surfactants serve two general purposes: to ensure proper mixing of all materials in the foam formulation; and, to reduce surface tension during the foaming process so as to allow the formation of a fine cellular structure within the foam [11]. Common surfactants which are used include Goldschmidt B-8404, B-8462, Air Products DC-5454, DC-198 and DC-193. Blowing agents are chemical substances that are widely used to generate gas needed to expand rubber, plastics and ceramics to make a foam. Blowing agents can provide a variety of useful properties to the foam being produced which include light weight, heat insulation, sound absorbency, elasticity, permeability, electrical insulation, texture, wood grain, and shock absorbency. Some common blowing agents which are

used in foam formulations include water, cyclopentane, and Genetron-141b. The catalyst and co-catalyst serve to speed up the reaction and the foaming process. Catalysts which are often used include DBTDL T-12, DABCO DMEA, and Niax A-1. Cross-linkers serve to enhance the mechanical strength and rigidity of the material. Many different cross-linkers have been used including glycerin, triethanolamine, sorbitol, water and trimethylolpropane (TMP) to name a few.

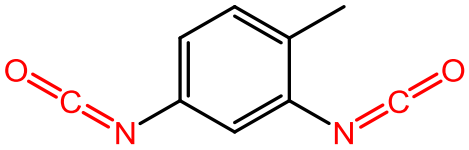

toluenediisocyanate (TDI)

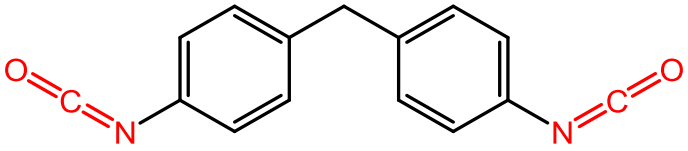

diphenylmethane diisocyanate (MDI)

Figure 1.3: Structure of diisocyanates.

As stated previously, the properties of polyurethanes are largely dependent on the functionality of the monomeric units used to produce it. Polyurethanes were first produced in 1937 by Otto Bayer and his coworkers and they represent a large family of polymers. Polyurethanes can be produced with a wide range of properties from soft flexible foams to hard rigid foams. As a result of this, polyurethanes are able to serve a purpose in many different applications.

There are five main areas of application for which polyurethanes are used. The first is in the mattress and furniture industry, which integrates flexible polyurethane foams into products like seat cushions. The automotive industry has many uses for both flexible and rigid polyurethane foams as well as elastomers. Flexible polyurethane foams are used for seat cushions in automobiles while rigid foams can be used as side insulation to help increase impact resistance. Elastomeric materials are primarily used for engineering components in vehicles. Another industry which makes good use of polyurethane foams is the consumer sector which is able to produce and sell products while utilizing all different types of polyurethanes. The construction industry is the largest consumer of polyurethane foams. These polyurethane rigid foams are good thermal insulator and are used for building insulation. The last main area of polyurethanes use, which is the second largest consumer of polyurethane foams, is the refrigeration engineering industry. The refrigeration industry primarily uses polyurethane rigid foam for the purpose of thermal insulation.

1.3. Synthesis of Polyols by the Thiol-Ene Reaction

Alternatives to petrochemical feedstock for the production of polyols have been explored within the field of scientific research. In recent years, polyols used for the synthesis of polyurethane foams have been prepared from bio-based materials which contain carbon-carbon double bond unsaturation. This has been accomplished by a radical process called the thiol-ene reaction [12]. A general scheme for the thiol-ene reaction is given in Figure 1.4. There has been a push towards utilization of bio-based

renewable starting materials for a variety of industrial applications due to the concerns which have arisen in recent years about sustainability of natural resources. One alternative to petrochemical feedstock which has been found is biomass from plant-derived resources because they are renewable raw materials which are capable of providing a large variety of starting material for monomers used to produce polymers. For example, the juicing and peeling industry produces bio-waste in the form of orange peels whose oil contains 90-95% limonene, a product which has been studied for its ability to produce environmentally-friendly polyols and polyurethane rigid foams [9]. Some other bio-based materials which have been used and explored include soybean oil, castor oil, starch and cellulose [13-16].

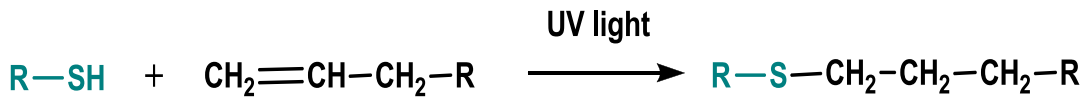

Figure 1.4: Thiol-ene reaction.

In recent years the thiol-ene reaction has been increasingly used to create polyols to prepare high yields of polyurethane rigid foams that reproduced in relatively short reaction times. Due to the near absence of by products, this reaction does not require an extra purification step in its process, adding to its wide spread use. These characteristics have produced thought that thiol-ene reactions may fall into the category of “click chemistry” reactions. The thiol-ene reaction has been used to prepare dendrimers, star

polymers and shape memory polymers for medical applications [17-20]. It has been used to prepare terpene-based thiols by reaction of H_2S with terpenes such as α-pinene, α- and γ-terpenine, terpinolene, 3-carene and pulegone which can then be further reacted with alcohol-containing alkene small molecules by a thiol-ene reaction to produce polyols [21]. Polyols have been prepared from the thiol-ene reaction of canola (rapeseed) oil with 2-mercaptoethanol which were further used to produce polyurethane foams [22].

1.4. Other Uses for the Thiol-Ene Reaction

The efficiency of the thiol-ene reaction has allowed it to flourish as a reaction used in a number of different scientific applications. A number of alkene-functionalized polymers have been studied using the thiol-ene reaction to couple different functional groups to the polymer backbone. This has been done using the thiol-ene coupling both photochemically and thermally in order to test the efficiency of the process under differing conditions [23]. From this aforementioned study, it was found that the photochemical version of the thiol-ene reaction proceeded with higher efficiency; it needed shorter reaction times before complete conversion was reached, and it was tolerant to many different mercaptans which were used as the coupling agents [23].

Thiol-ene reactions have sparked interest for their use as a potential surface functionalizing method for biomolecules. The ability to immobilize biomolecules at specific locations on the surface of solid supports is crucial to many biochip applications [24]. The success of the thiol-ene reaction for its use in this particular field is a result of

its specificity for alkenes. It was found the reaction can be carried out photochemically in an aqueous buffer medium without interfering with normal biochemical processes [24].

Many researchers have used the thiol-ene reaction for a variety of different purposes. An example study is one in which bio-based telechelics were prepared by a one-pot thiol-ene "click" process which consisted of step-growth polymerization using 3,6-dioxa-1,8-octanedithiol and end-group postpolymerization modification with differing thiols [25]. This method was applied to the allyl ester of 10-undecenoic acid, which is a bio-based material. A series of telechelics were prepared which had molecular weights ranging from 1000-3000 g mol^{-1} and which had hydroxyl, carboxyl and trimethoxysilyl groups at their polymer terminus. The 10-undecenoic acid based telechelic diols which were prepared, were then reacted with 4,4'-methylenebis(phenylisocyanate) (MDI) and 1,4-butanethiol chain extender to produce multiblock poly(ester urethane) [25].

1.5. Purpose of this Research

Presented here is the overall objective of the experiment which will serve as the primary topic of discussion from here on. Many bio-based materials have been tested for potential use within the application of polyurethane commercial products. In this work, the testing of two bio-based materials which have not been used previously for the purpose of producing polyurethane foams was accomplished. As stated earlier, polyurethanes are used for a variety of different applications within the commercial sector. The goal of this study is to introduce one or two new bio-based materials which could replace material platforms used in the polyurethane commercial sector. A few

sources of polyols used to produce polyurethanes within the commercial sector include soybean oil, linseed, castor oil, sugar/glycerol, and polyethylene oxide [26-29].

The two materials which were experimented with in this study are β-caryophyllene and α-phellandrene (Figure 1.5). β-caryophyllene is found in the oils of many different plants including rosemary, hops, cloves and cannabis. The compound is also found in high amounts in the *Piper nigrum* plant which is used to make black pepper. It is known as a cannabinoid which acts selectively on the CB2 receptors in the human body. As a result of this fact, β-caryophyllene has been studied within the medical field extensively as a potential treatment for many inflammatory diseases such as arthritis, bladder cystitis, multiple sclerosis and HIV-associated dementia. This particular compound has the potential to effectively combat the aforementioned conditions without the added effect of the marijuana high which is associated with tetra-hydrocannabinol (THC) and the CB1 receptors. This makes β-caryophyllene especially desirable for use within the medical field [26].

The second material which was tested in this study, α-phellandrene, can be isolated naturally by distillation of the leaves of the tree, *Eucalyptus radiate*. Other known sources include the essential oil of *Eucalyptus dives*, the oil in water fennel, and Canada balsam oil. It is found as a primary constituent in *Ridolfia Segetum* and *Elemi* while it is a minor constituent in eucalyptus, melaleuca, fennel and ginger. The phellandrenes are commonly used in fragrances because they tend to have pleasing aromas.

Source for α-phellandrene

Source for β-caryophyllene

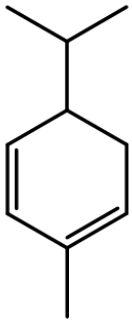

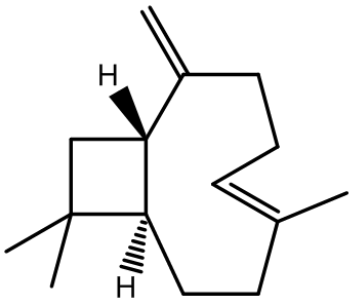

Figure 1.5: Structure and sources of α-phellandrene and β-caryophyllene.

The two aforementioned materials were used in the first step of the experiment to produce bio-based polyols which were used to produce polyurethane foams. Polyols were prepared by the photochemical variety of the thiol-ene reaction using the two hydroxyl group containing thiols, 1-thioglcerol and 2-mercaptoethanol. 1-thioglycerol has two equivalents of hydroxyl groups per molecule while 2-mercaptoethanol has one equivalent of hydroxyl group per molecule. Polyols containing various mole ratios of 1-thioglycerol and 2-mercaptoethanol were synthesized to see the effect of functionality on the properties of polyurethanes. Each bio-based material contains two alkene functional groups within their molecular structure. Therefore, in each of the polyol-

producing experiments, there were two equivalents of thiol added to the reaction mixture to ensure that the addition of a thiol group occurred for both of the alkene groups within the structure of each of the bio-based materials studied. In one of the experiments, employed for both α-phellandrene and β-caryophyllene, two equivalents of 1-thioglycerol were used for the photochemical thiol-ene reaction. Yet another experiment employed the use of one equivalent of 1-thioglycerol and one equivalent of 2-mercaptoethanol to be added to both of the bio-based materials of study. The third experiment which was conducted for each of the alkene-containing materials employed two equivalents of 2-mercaptoethanol for the photochemical thiol-ene reaction to produce bio-based polyols. Once all polyols were synthesized in the manner described above, tests were run on all the polyols to determine a variety of different properties. The properties which were determined for all polyols included: hydroxyl number, acid value, FT-IR analysis of functional groups, viscosity, and gel permeation chromatography (GPC). Finally, these characterized polyols were used for the preparation of polyurethane foams which were tested against an industrial foam reference in properties which include closed cell content, density, thermal stability, glass transition temperature, cell morphology and mechanical property.

CHAPTER II

EXPERIMENTAL DETAILS

2.1. Starting Materials

For the synthesis of polyols and polyurethanes, the following compounds were used as received.

α-phellandrene (≥85%): purchased from Sigma-Aldrich, 100 g, CAS# 99-83-2, MW: 136.23 g/mol, density: 0.845 g/mL at 25°C

β-caryophyllene (≥80%): purchased from Sigma-Aldrich, 1 kg, CAS# 67-44-5, MW: 204.35 g/mol, bp: 129-130°C, density: 0.901 g/mL at 25°C

α-thioglycerol (≥95.0%): purchased from TCI, 500 g, MW: 108.16 g/mol, CAS# 96-27-5, density: 1.25 g/mL

2-hydroxy-2-methylpropiophenone (>96%): used as photoinitiator for polyol synthesis experiments, purchased from TCI, 500 g, CAS# 7473-98-5, MW: 164.20 g/mol, density: 1.08 g/mL

2-mercaptoethanol (99%): purchased from Acros Organics, 1 L, CAS# 60-24-2, MW: 78.13 g/mol, density: 1.110 g/mL,

Rubinate M: purchased from Huntsman Polyurethanes, The Woodlands, TX, Lot# GE014970, 19 kg, EW: 135 g/functional group

Jeffol SG-360: purchased from Huntsman Polyurethanes, The Woodlands, TX, Glycerol/PO Polymer CAS# 25791-96-2, Sucrose/PO Polymer CAS# 9049-71-2, Lot# GE000793, 3.8 kg

Niax A-1: purchased from Huntsman, The Woodlands, TX, Lot# 4F519, CAS# 3033-62-3, 25265-71-8, 0.5 kg

DABCO T-12 (dibutyltin dilaurate) 95%: purchased from Sigma-Aldrich, CAS# 77-58-7, FW: 631.56, density: 1.066, 100 g

Silicon B-8404: purchased from Degussa Goldschmidt Chemical, Batch# HW27A11463

2.2. Synthesis of Polyols

The polyols were synthesized using thiol-ene click chemistry. They were synthesized in various mole ratios in order to have a range of materials with varying hydroxyl numbers (OH#). The details of the experimental parameters are given in Table 2.1. In general, the required amounts of starting materials were added into a 125 mL glass jar. In this mixture, the required amount of 2-hydroxy-2-methylpropiophenone was added as the photoinitiator. Once all components were added, the reaction mixture was stirred under a photochemical lamp (UVLS-28 EL Series) at a wavelength of 365 nm. All the experiments were carried out at room temperature for 8 hr. The chemical structures of the synthesized polyols are given in Figure 2.1. The synthesized polyols were

characterized using various methods. Hydroxyl number is a critical property which is necessary to characterize polyols and it is defined as the mg of KOH equivalent to the hydroxyl content in 1 g of a polyol sample. The theoretical hydroxyl numbers of the polyols were calculated and compared with the experimentally determined hydroxyl numbers. The theoretical hydroxyl numbers were calculated using the equations give below:

$$Equivalent\ Weight\ (EW) = \frac{Molecular\ Weight\ (MW)}{Functionality\ (f)} = \frac{56110}{OH\#}$$

$$OH\# = \frac{56.11 * 1000}{MW}$$

$$MW = \frac{f * 56110}{OH\#}$$

2.3. Characterization of Polyols

The synthesized polyols were characterized using various available techniques. The phthalic anhydride/pyridine (PAP) and toluene sulfonyl isocyanate (TSI) methods were used to determine the hydroxyl number of the polyols. Hydroxyl number is defined as the mg of KOH equivalent to the hydroxyl content in 1 g of a polyol sample and is an essential property for one to know before developing foam formulations. The details of these two methods are given in **Section 2.3.1** and **Section 2.3.2**.

Table 2.1: Experimental details for the synthesis of polyols.*

Polyols (mol ratio)	Amount of AP used (g)	Amount of BC used (g)	Amount of TG used (g)	Amount of ME used (g)	Amount of photoinitiator used (g)
AP-TG (1:2)	27.13	0	36.65	0	2.85
AP-ME-TG (1:1:1)	24.28	0	16.38	11.84	2.50
BC-TG (1:2)	0	49.06	41.55	0	3.17
BC-ME-TG (1:1:1)	0	39.26	16.65	12.08	2.55

***Note:** AP- α-phellandrene, BC- β-caryophyllene, TG- α-thioglycerol, ME-2-mercaptoethanol.

2.3.1. Phthalic Anhydride/Pyridine (PAP) Method

To determine the hydroxyl number using the PAP method, 0.5 g of the polyol was added into two separate 100-mL glass bottles. A control experiment was also performed without the polyols. 10 mL of PAP reagent was added accurately by pipette into each of the bottles (the two polyol sample bottles and the blank bottle) under stirring with the help of a magnetic stirrer. The glass bottles were sealed and heated at 100°C for 70 minutes. This heating was coupled with shaking of the bottles to mix at 15, 30, 45 and 60 minutes during the experiment.

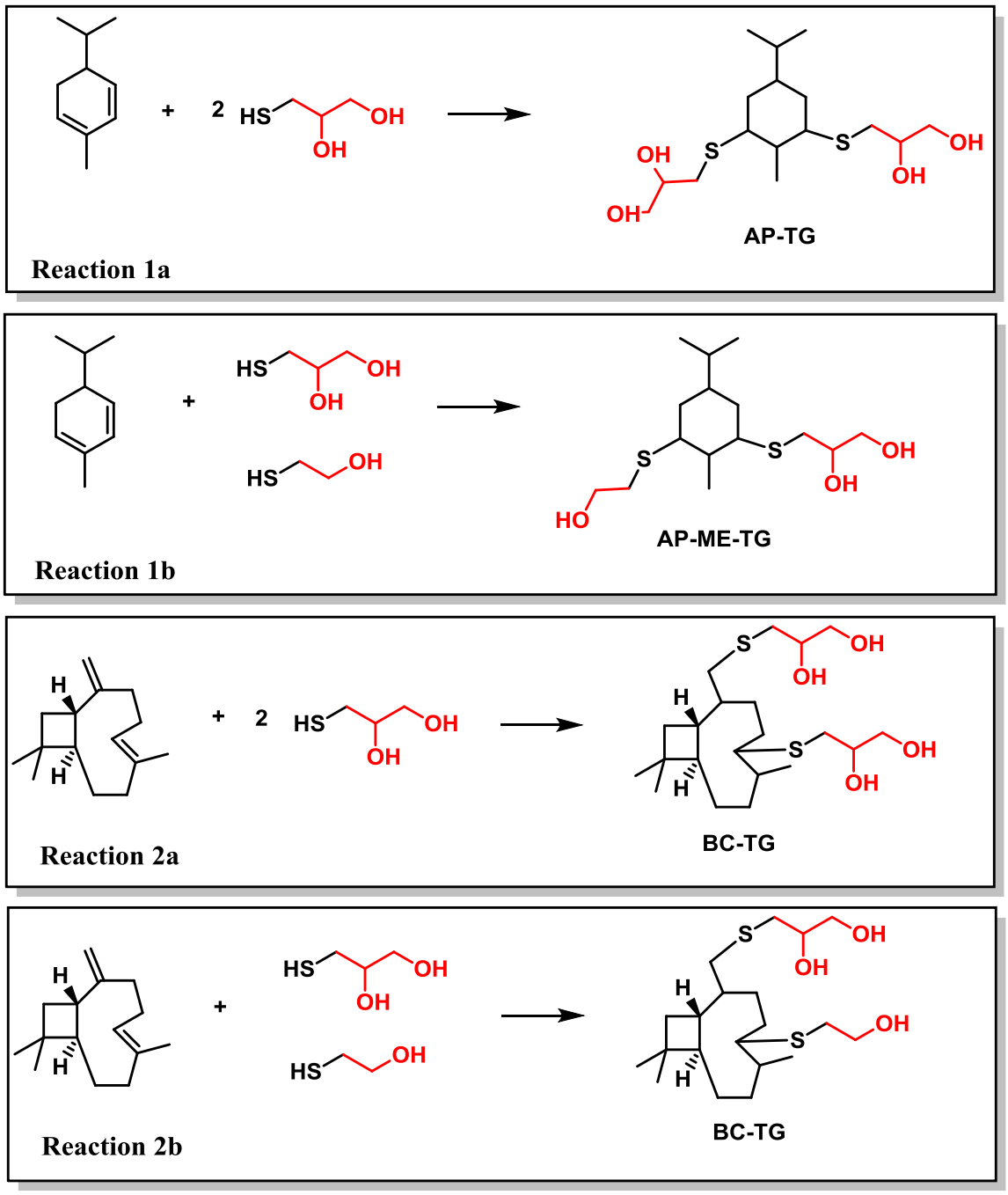

Figure 2.1: Chemical structure of the synthesized polyols.

After 70 minutes, the bottles were taken out of the oven and were allowed to cool to room temperature naturally. After cooling to room temperature, 10 mL of HPLC grade water was added accurately by pipette to each of the bottles and each bottle was then stirred at room temperature for 10 minutes. After this, 20 mL of isopropanol containing phenolphthalein indicator was added accurately by pipette to each of the bottles and the mixtures were stirred at room temperature for 5 minutes. Each of the samples was then titrated against 1.000 N NaOH. Each experiment was repeated once and an average value was determined for the hydroxyl number. The hydroxyl number of the polyols was then calculated using the equation below.

$$OH\# = \frac{56.11(v_0 - v)}{w} + AV$$

Note: v_0 = volume of 1.000 N NaOH used to titrate the blank, v= volume of 1.000 N NaOH used to titrate the sample mixture, w= weight of sample used, AV= acid value (which is defined as the mg of KOH required to neutralize the free acid component in 1 g of a polyol) of the sample

2.3.2. Toluene Sulfonyl Isocyanate (TSI) Method

The TSI method based on ASTM E 1899-97 standard was used to determine the hydroxyl number of all the polyols except for polyol AP-TG for which it was presumed that a solubility issue was present which made it incompatible with the TSI reagent. It was presumed that a solubility issue existed for all other polyols in the PAP reagent.

The weight of sample polyol used for the experiment was determined by using the equation below. A few milligrams of the polyol were weighed precisely into a 100 mL beaker. After this, 3 mL of toluene and 7 mL of acetonitrile were added accurately to the sample followed by slow stirring until the polyol was completely dissolved.

$$W\ (g) = \frac{40}{expected\ OH\#}$$

After this, 10 mL of TSI reagent was added to the beaker accurately by pipette and the mixture was stirred for 5 minutes. In this, 0.5 mL of HPLC grade water was added via syringe to destroy excess TSI reagent followed by 1 minute of stirring. Then 30 mL of acetonitrile was added, at which point the sample was ready to test. The sample was titrated against standardized 0.1 N Bu_4NOH using an automatic titration system Titrando 888.

The polyols were further characterized for an acid value (AV) based on IUPAC 2.201 standard. The acid value of a compound is defined as the mg of KOH that is required to neutralize the free acid component of 1 g of a compound.

2.3.3. Acid Value

For the acid value determination, a polyol was weighed out into a 100 mL beaker and was dissolved in about 30 mL of a solvent mixture of 1:1 (v/v) isopropanol/toluene in the presence of phenolphthalein indicator. A stir bar was added to the solution and the mixture was stirred until the polyol was completely dissolved. The solution was then titrated against 0.1 N potassium hydroxide to the end point which was indicated by the

presence of a light pink color which persisted for 30 seconds. The titration was performed using a 719 S Titrino instrument. The acid value was calculated by the equation below, where 56.1 is the molecular weight of potassium hydroxide, T is the normality of the potassium hydroxide solution used to titrate the solution, V is the volume of 0.1 N KOH which was required to reach the end point of the titration, and w is the weight of the polyol sample which was used to prepare the solution which was tested for AV.

$$AV = \frac{56.11 * T * V}{w}$$

2.3.4. Gel Permeation Chromatography (GPC)

All the synthesized polyols were characterized using gel permeation chromatography (Waters Corporation, Milford, MA, USA). The columns of the GPC instrument were kept pressurized to between 695 and 700 psi. A sample of 1-2 drops of polyols was dissolved in 1 mL THF. The resulting solution was drawn up into a syringe and a 0.2 μm filter was attached to the syringe. The solution was filtered while being dispensed into a GPC vial. The GPC vial was placed into the GPC instrument for a run. While the GPC was running, a tube was hooked up to the THF bottle which needed to be placed in the waste container. After GPC runs were completed, this tube was placed back into the THF bottle. Before running GPC, the ports which contained the samples which were to be run were defined on the keypad of the GPC instrument.

2.3.5. Fourier Transform Infrared Spectroscopy (FT-IR)

The polyols were further characterized by FT-IR spectroscopy (Perkin Elmer, Ultra 2). The sample for FT-IR was prepared by placing 1-2 drops of polyols on the crystal of the FT-IR machine. This step was done after collecting a background spectrum for the instrument. The sample was pressed to a force of 50 relative units while the spectrum for it was being collected. Four sans were done for each sample. FT-IR analysis was used to determine the bond vibrations of the polyol molecules which were based on the frequency of the bond vibrations. The method can also be used to assess the progress of a reaction due to the fact that if functional groups present within the starting material were targeted for transformation during the reaction, the peaks corresponding to those functional groups will disappear after the completion of the reaction. For instance, if an alkene functional group was targeted for reaction with a thiol group as is the case for the synthesis of polyols in this study, the IR spectrum of the bio-based starting material will show a characteristic peak for alkene C-H bonds within the 3000-3100 cm^{-1} region. After reaction with thiol group takes place, this particular peak should disappear from the IR spectrum of the polyol product. If this is in fact the case with the IR spectrum of the polyol, then one would know that the reaction went to completion. The completion level of polyol formation can also be assessed by looking for the appearance of a broad band in the 3300-3600 cm^{-1} region of the IR spectrum which would indicate an alcohol originating from the hydroxyl groups present within 1-thioglycerol and 2-mercaptoethanol.

2.3.6. Viscosity Measurements

Viscosity is defined as the resistance to flow for a material. Viscosity of a polyol can give a good measure of the extent of intermolecular forces present. The viscosity of a material is also able to provide a measure of how easily it will be processed. Higher viscosity polyols tend to be harder to process than those which have lower viscosity and as a result they generally require a higher energy input in order for them to be able to flow as needed for processing. The viscosity of the synthesized polyols were measured using an AR 2000 ex rheology instrument. Viscosity of all the polyols was measured at 25 ^{o}C. Viscosity of the polyols was collected using the continuous ramp shear stress method with a cross-head speed which went up to 100 Hz for low viscosity polyols and up to 200 Hz for high viscous polyols.

2.4. Preparation of Polyurethane Rigid Foams

Once all polyols were characterized, foam formulations were generated to prepare polyurethane foams. The foams were produced by mechanically mixing appropriate amounts of polyols, diisocyanates, catalyst, surfactant and blowing agent until a homogeneous mixture was achieved and the foam began to rise. The amount of isocyanate (Rubinate M, index 105) in each formulation was based on equivalent weight of polyols and distilled water:

$$w_i = Ew_i \cdot \left(\frac{w_p}{Ew_p} + \frac{w_{pc}}{Ew_{pc}} + \frac{w_{water}}{Ew_{water}}\right)$$

where w_i, w_p, w_{pc} and w_{water} are the weights of isocyanate, polyols, commercial polyols and water, respectively. Ew_i, Ew_p and Ewp_c, are the equivalent weights of isocyanate and polyols, and Ew_{water} = 9 is the hydroxyl equivalent weight of water.

Once rising started, various times were recorded for each foam which was prepared. The times which were recorded include: mix time, cream time, tack-free time and rise time. The mix time is the time during which mechanical stirring was performed. Cream time is defined as the time at which the mixture changed from an apparently free flowing liquid to the beginning of the foaming of the mixture. Tack-free time is the time at which the foam ceases to have a sticky texture and becomes hard. The rise time is the time at which the foam stops rising upwards as the mixture is undergoing the foaming process. Once all times mentioned above were recorded, the foams were allowed to cure for 7 days under standard conditions of ambient temperature and atmospheric pressure.

2.4.1. Synthesis of Rigid Polyurethane Foams Composed of a 50/50 Blend of Synthesized Polyols and Jeffol SG-360

Polyurethane rigid foams composed of a 50/50 (by weight) blend of our synthesized polyols and commercial available polyols (Jeffol SG-360) were prepared. The details of the formulations are given in Table 2.2. Four foams were synthesized in this blend series. In general, all the chemicals except Rubinate M was added in to 400 mL plastic cups and were mixed using a Delta ShopMaster mechanical rotary stirrer. After mixing, the Rubinate M was added to the mixture via syringe followed by mechanical stirring. Mechanical stirring was coupled immediately with the recording of characteristic

times which are typical of polyurethane foaming reactions. All of these times were recorded using a digital timer. The purpose of synthesizing blend polyurethanes was to examine whether foams made with the novel bio-based polyols prepared in this study could be as good as polyols already in use and known to give foams possessing good properties. After completion of the reaction (when raise in foam stopped), pictures were taken of each of the foams and then the foams were allowed to cure for 7 days at room temperature and atmospheric pressure.

Table 2.2: Rigid foam formulations of 50/50 blends by weight (g).

Chemicals	Foam 1	Foam 2	Foam 3	Foam 4
BC-TG	10.00	0	0	0
BC-ME-TG	0	10.02	0	0
AP-TG	0	0	10.00	0
AP-ME-TG	0	0	0	10.00
Jeffol 360	10.03	10.02	10.05	10.03
B-8404	0.40	0.40	0.41	0.40
Niax A-1	0.12	0.12	0.12	0.12
T-12	0.04	0.04	0.03	0.03
Water	0.82	0.80	0.81	0.80
Rubinate M (index 105)	32.82	31.20	35.62	34.30

2.4.2. Synthesis of Rigid Polyurethane Foams Composed of 100% of the Synthesized Polyols

In addition to preparation of blend polyurethane foams, rigid polyurethane foams using 100 % of the synthesized bio-based polyols were prepared. For the preparation of these rigid polyurethane foams, the same procedure was adopted as described above. The details of the formulation are given in Table 2.3.

Table 2.3: Rigid polyurethane foam formulations using 100% synthesized polyols.

Chemicals	Foam 5	Foam 6	Foam 7	Foam 8
BC-TG	20.00	0	0	0
BC-ME-TG	0	20.00	0	0
AP-TG	0	0	20.00	0
AP-ME-TG	0	0	0	20.00
B-8404	0.40	0.40	0.40	0.40
Niax A-1	0.12	0.12	0.12	0.12
T-12	0.04	0.04	0.03	0.03
Water	0.82	0.80	0.81	0.80
Rubinate M (index 105)	39.55	34.36	44.58	38.80

In addition to these polyurethane foams, a reference rigid polyurethane foam was prepared to compare the foam properties. The reference foam using Feffol SG-360 was prepared in a similar way to all other foams. The formulation for the reference polyurethane foam is given in Table 2.4. Jeffol SG-360 is a commercial polyol which is

already used for preparation of polyurethanes in various industries. All the properties of the foam were compared with the reference rigid polyurethane foam to assess whether any of the foams which contained the bio-based polyols chosen for use in this study could serve as a reasonable replacement for the Jeffol SG-360 foam.

Table 2.4: Formulation for the reference polyurethane foam.

Reference Foam	Wt (g)
Jeffol SG-360	20.00
Silicone B-8404	0.40
Niax A-1	0.11
T-12	0.04
Water	0.80
Rubinate M (index 105)	30.78

2.5. Characterization of the Rigid Polyurethane Foams

The rigid polyurethane foams which were synthesized in this study were characterized for several different properties which are essential for assessment of the viability of polyurethane foams for various applications. These properties include 10% compression strength, closed cell content, apparent density, thermal stability, glass transition temperature and morphology.

2.5.1. Compression Strength

A Q-Test 2-tensile machine (MTS, USA) equipped with compression fixture was utilized in foam compressive properties determination. The test was done according to standard ASTM 1621, on foam of about 50x50x25 mm dimensions (cut out of the top part of the foam with respect to the direction of rise). A 1250 N cell was used for the compression tester during the performing of 10 % compression strength tests. The cell was calibrated prior to testing of foams. Rigid polyurethane foam was placed between two parallel plates (25.4 mm distance), and the force required to compress the foam in the direction of the rise at a constant rate (30mm/min, max. load cell 1250N) was measured. Applied force vs. the displacement of the foam was recorded as a stress-strain curve. Compressive strength values were recorded at 10 % strain as well as any other yield points which may have occurred prior to 10 % strain in the stress/strain curves of the foams.

2.5.2. Closed Cell Content

Closed cell content of the foams was measured based on the ASTM 2856 test method. Testing was performed using a HumiPyc pycnometer. The foam for the closed cell content measurements was cut in the cylindrical form in the foam's direction of rise. The blocks were cut into dimensions of 1 inch in height and 2 inches in diameter. Measurements of the blocks from each prepared foam were taken and precise values for the dimensions were obtained. The surface dust absorbed during cutting the foams was blown off prior to closed cell content measurement. Before testing, a N_2 line attached to

the HumiPyc Model 2 NEVA Series volumetric analyzer instrument was opened up and the pressure was kept at approximately 20 psi. The HumiPyc software was used to measure the volume of the empty chamber. After the volume of the chamber was determined precisely, each foam was submitted to the HumiPyc volumetric analyzer for closed cell content determination. After maximum of 5 runs, the results were averaged. Closed cell content of the foam was reported in %.

2.5.3. Apparent Density

The apparent density of foams was determined according to standard test method for apparent density of rigid cellular plastics (ASTM D 1622). The apparent density of each of the foams was calculated as an average of the densities of the top and middle portions of the foam in the direction of rise of the foam. For this, a cylindrical foam with a diameter of about 4.6 cm and a height of about 3 cm was cut out. The weight of the foam was measured on a balance of ± 5 mg precision. After the dimensions were measured to ± 0.1 mm precision, the density was calculated.

2.5.4. Thermogravimetric Analysis (TGA)

Thermogravimetric measurements of the rigid polyurethane foams were performed on a TGA instrument (model Q50, TA Instruments, New Castle, DE, USA). All the experiments were carried out under a nitrogen atmosphere (60 mL/min) with a heating rate of 10°C/min from room temperature to 600°C. Weight loss and derivative of

weight loss as a function of temperature were recorded and analyzed using Universal Analysis software from TA instruments.

2.5.5. Dynamic Mechanical Analysis (DMA)

The glass transition temperatures of the rigid polyurethane foams were measured using a Dynamic Mechanical Analyzer (DMA 2980 from TA instruments). A rectangular shape foam was cut out with the longest dimension along the direction of the foam rise. The rectangular shaped foam (about 15 mm x 6 mm x 2 mm) was clamped in a mechanical oscillator. Measurements were performed with heating rate of 3°C/min in a temperature range from 30°C to 250°C under the single frequency of 10 Hz. Plots of the elastic modulus, loss modulus and tan δ versus temperature were acquired via TA Universal Analysis software.

2.5.6. Microstructural Characterization of the Foams

The microstructure and morphology of the polyurethane foams were observed at 490 µm resolution via scanning electron microscopy (SEM) Phenom G2 Pro SEM (Netherlands). The foams were gold coated in a 108 Sputter Coater (Kurt J. Lesker Co.) before loading to SEM chamber to avoid the charging effect during imaging. The descriptions of the sizes of the cells for foams present in the **Results and Discussion** section are based on how the sizes of the cells compared relative to one another by simple visualization of the microstructural picture.

CHAPTER III

RESULTS AND DISCUSSION

3.1. Polyol Data and Discussion

The synthesized polyols were characterized for hydroxyl number, viscosity, acid value, GPC and FT-IR. The results for the properties of hydroxyl number, acid value and viscosity are presented in Table 3.1. The equivalent weights of the polyols were calculated based on the hydroxyl number which was determined for each polyols experimentally. The values obtained for the equivalent weight of each polyol were used in the calculations of isocyanate amount for preparation of rigid polyurethane foams.

3.1.1. Hydroxyl Number

It can be seen in Table 3.1 that the experimentally determined hydroxyl numbers are lower than that of the theoretical hydroxyl numbers. This suggests that the reactions were not 100 % completed as also indicated in the GPC analysis of the polyols. Potential reasons for this result could be the relatively low reactivity of second alkene groups present in the α-phellandrene and β-caryophyllene molecules.

Table 3.1: Some of the properties of the polyols.

Polyol	Hydroxyl number (calculated) (mg KOH/g)	Hydroxyl number (experimental) (mg KOH/g)	Equivalent weight (g/OH equivalent)	Acid Value (mg KOH/g)	Viscosity (Pa.s)
AP-TG	632.97	554.05	88.64	10.28	0.6161
AP-ME-TG	520.23	499.71	107.85	13.35	0.1567
BC-TG	533.43	440.96	105.81	7.04	20.35
BC-ME-TG	430.83	376.99	130.23	6.30	3.78

In the β-caryophyllene molecule, there is a terminal alkene which should react quite readily in almost quantitative amounts. However, there is a tri-substituted alkene group also in the molecule which is less reactive and therefore, could have had significant amounts left unreacted at the end of the reaction time. The reduced experimental hydroxyl number values within the β-caryophyllene series of polyols could have been largely due to some of this particular functional group being left unreacted, as can be seen from the relatively high differences in experimental hydroxyl number and the calculated hydroxyl number for BC-TG; 533.43 mg KOH/g versus 440.96 mg KOH/g and for BC-ME-TG; 440.83 mg KOH/g versus 376.99 mg KOH/g. The larger separation of hydroxyl number values for polyol BC-TG could be due to the fact that 1-thioglycerol is a more sterically hindered thiol functional group which could have resulted in reduced reactivity towards

the alkene groups. This can be explained by comparing the results with that of polyol BC-ME-TG.

There is less separation of the hydroxyl number values present in BC-ME-TG than there is in polyol BC-TG. This can be explained by the fact that 2-mercaptoethanol was used in the synthesis of BC-ME-TG which has a less sterically hindered thiol functional group than the one present in 1-thioglycerol. As a result of this, 2-mercaptoethanol is more reactive than 1-thioglycerol and had a more complete reaction with alkene group than 1-thioglycerol. This resulted in the reduced separation of hydroxyl number values of experimental versus calculated with polyol BC-ME-TG than the separation between the values which resulted for polyol BC-TG.

Reduced experimental hydroxyl number values were also found within the α-phellandrene series of the polyols compared with the theoretical hydroxyl number values which were calculated for both AP-TG and AP-ME-TG. Within the α-phellandrene molecule, there is a presence of conjugation of the alkene functional groups which enhances the stability of these functional groups significantly due to the resonance effect which results in delocalization of the resulting radical when a thiol group reacts with one of the alkenes present within the molecule. The effect of reduced reactivity between 1-thioglycerol versus 2-mercaptoethanol is also present within the α-phellandrene series of polyols. The separation in the hydroxyl number values between the experimental and the calculated hydroxyl numbers in the α-phellandrene series of polyols overall, is less than the separation which is present in the β-caryophyllene series of polyols. As expected, the separation in the hydroxyl number values was less in AP-ME-TG: 520.23 mg KOH/g versus

499.71 mg KOH/g than in AP-TG: 632.97 mg KOH/g versus 554.05 mg KOH/g which is due to the increased reactivity of 2-mercaptoethanol thiol group over the 1-thioglycerol's thiol group. The increased separation in the hydroxyl number values for the β-caryophyllene polyols versus the α-phellandrene polyols could be due to the fact that the tri-substituted alkene present in β-caryophyllene is more stable and, therefore, less reactive, than either of the alkenes present in α-phellandrene.

3.1.2. Acid Value

Acid values of all the polyols synthesized ranged from 6.30 to 13.35 mg KOH/g. It was determined that the acid values for the β-caryophyllene based polyols were less than that of the α-phellandrene based polyols. The acid values of the polyols from the β-caryophyllene series were relatively similar. The acid value for the BC-TG and BC-ME-TG polyols was determined to be 7.04 and 6.30 mg KOH/g, respectively. The slightly lower acid value for polyol BC-ME-TG could be due to the fact that the reaction of the thiol group was more complete in the synthesis of BC-ME-TG than in BC-TG due to steric reasons. The sulfhydryl group is relatively acidic compared to the hydroxyl groups which are present in 1-thioglycerol and 2-mercaptoethanol and, therefore, it contributes more significantly to the acid value of the polyols. In the α-phellandrene series of polyols, the acid values determined were relatively higher with AP-TG having a value of 10.28 mg KOH/g while AP-ME-TG had a value of 13.35 mg KOH/g.

3.1.3. Viscosity of the Polyols

Viscosity values were determined for each of the polyols based on the parameter of shear rate. It was found that, overall, the polyols from the β-caryophyllene series were much more viscous than the polyols in the α-phellandrene series. In the β-caryophyllene based polyols, BC-TG had a viscosity of 20.35 Pa.s which was, by far, the highest of any polyols which was synthesized in this study. BC-ME-TG had the second highest viscosity with a value of 3.78 Pa.s at 25 ^{o}C. The highest viscosity of polyol BC-TG can be attributed to the numerous amount of hydrogen bonds which can be formed between polyol molecules. The addition of 1-thioglycerol to each of the alkene groups present in β-caryophyllene creates a polyol which has a hydroxyl functionality of four. The viscosity of the polyol BC-TG could also be enhanced by the irregular shape of the molecule restricting the ability of neighboring BC-TG molecules to slide past one another. The reduced viscosity of BC-ME-TG compared with BC-TG could be due to the fact that the reduced functionality created by using an equivalent of 2-mercaptoethanol creates less opportunities for hydrogen bonding between polyol molecules. The possibility of multiple isomers from the synthesis of BC-ME-TG could also have created more diversity in the structures of the polyol, resulting in less packing and, therefore, more space for the neighboring polyol molecules to slide past one another.

Viscosity values of the polyols in the α-phellandrene series were significantly less than what was determined for the β-caryophyllene series of polyols. Polyol AP-TG had a viscosity value of 0.6161 Pa.s while AP-ME-TG had a value of 0.1567 Pa.s. The low values for viscosity for each of the polyols in the α-phellandrene series can perhaps be attributed

to irregularity and variety in the structure of the polyols. From the synthesis of each of the polyols in the α-phellandrene series, it is clear that a mixture of isomers can potentially be formed in each case. The resonance effect which is present upon the addition of a single thiol group to the conjugated system in α-phellandrene opens up the opportunity for a second thiol group to add in one of two places. Due to the variety which may be present in the structure of the α-phellandrene series polyols, it is possible that inefficient packing of the polyol molecules may be present which could be causing the intermolecular space to be fairly large making it easier for the polyol molecules to slide past one another. This effect could potentially explain the low viscosity of both of the polyols within the α-phellandrene series. It was found, as one would expect, that the viscosity of polyol AP-TG (0.6161 Pa.s) was higher than that of AP-ME-TG (0.1567 Pa.s). The reason for the higher viscosity of AP-TG is the fact that this polyol has a higher average functionality of hydroxyl groups than AP-ME-TG. Due to this fact, there is more opportunity for hydrogen bonding in AP-TG than in AP-ME-TG which creates stronger intermolecular bonding in AP-TG, restricting the separation which can occur between polyol molecules.

3.1.4. Gel Permeation Chromatography (GPC)

Figure 3.1 shows the GPC curves for polyol AP-TG and its starting materials. As seen, there is some unreacted 1-thioglycerol in the synthesized polyol. It can be seen from looking at the peak at approximately 41 min in the polyol, there is some unreacted α-phellandrene in the synthesized polyol. Looking at the AP-TG curve corresponding to the

product, one can observe slight amounts of higher molecular weight species from the peak at approximately 37 min and a lower molecular weight species at approximately 38 min while the in-between molecular weight species shown by the peak at approximately 37.8 min makes up the bulk of the product which was formed in the reaction. Therefore, it can be concluded that a distribution of products were formed in the synthesis; however, the identity of the chemical species which were formed was not a topic that was explored.

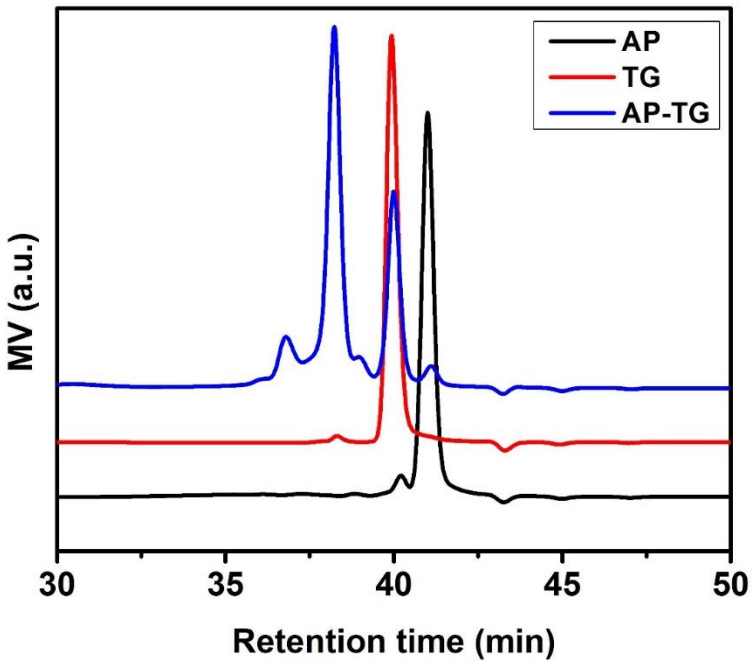

Figure 3.1: GPC curve of the AP-TG polyol and its starting materials.

The GPC curves of polyol AP-ME-TG and its starting materials are shown in Figure 3.2. It can be seen from the polyol curves that peaks at 40 min and 41.8 min are the unreacted 1-thioglycerol and 2-mercaptoethanol, respectively. It can be observed from the peak at 41.5 min of retention time that there is a slight amount of unreacted α-

phellandrene in the product. In the product curve AP-TG-ME, the lower retention times from 37 to 38.5 min, there is a distribution in the molecular weights of the products which were formed during the synthesis of this polyol. There is a small contribution from the larger molecular weight species at 37 min retention time while the middle and lower molecular weight species at 37.6 and 38.5 min retention time appear to make up the bulk of the polyol product.

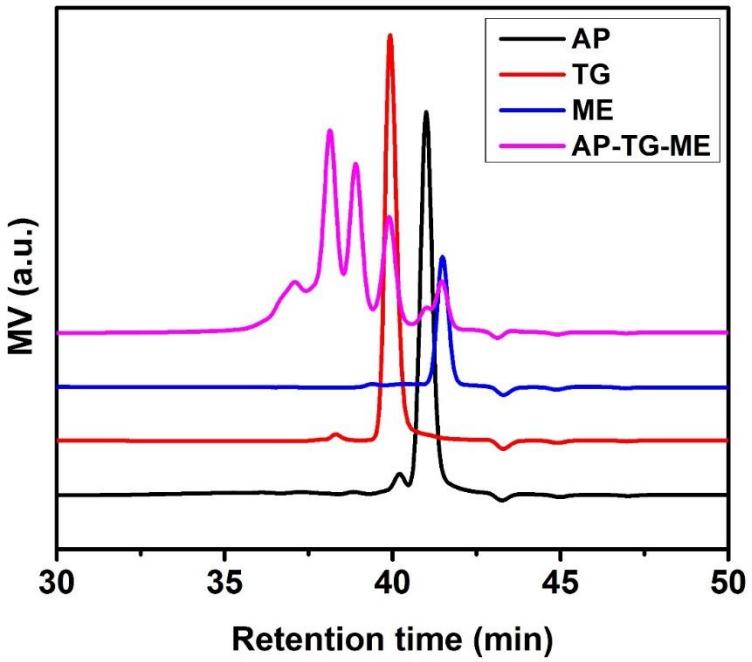

Figure 3.2: GPC curve of the AP-ME-TG polyol and its starting materials.

Figure 3.3 shows the GPC curves for the BC-TG polyol and its starting materials. As seen, the peaks at approximately 40 min retention time in the BC-TG polyol curve are due to unreacted starting materials. The peaks for both starting materials β-caryophyllene and 1-thioglycerol appear at very similar retention times and, therefore, it cannot be

determined by GPC alone exactly which starting material of the two was left unreacted in the final product. It is hypothesized that the peak at approximately 40 min retention time in the product curve, BC-TG, is due to a combination of both unreacted β-caryophyllene and 1-thioglycerol. In the BC-TG polyol curve, it can be seen that there is a higher molecular weight species at approximately 36.5 min retention time, which serves as a minor contributor to the polyol product while the primary contributor is the lower molecular weight species which has a peak appearing at 37.5 min retention time. The chemical structure of the species contributing to these aforementioned peaks was not determined because the research conducted here was a study in the feasibility of using the materials mentioned earlier for an industrial process to make polyurethanes at a reduced cost. All of the differing isomers which can be formed from the thiol-ene reaction with β-caryophyllene and α-phellandrene contain hydroxyl groups which can form urethane linkages in a polymer network. Due to this, it was not deemed necessary to obtain pure compounds. Purification of materials requires an extra cost which would not be desirable for industry when making the case for the use of these novel bio-based polyols.

The GPC curves of the BC-TG-ME polyol and the starting materials from which it is derived are shown in Figure 3.4. It can be seen from the peaks at 40 min retention time in the curves that there is a slight amount of unreacted starting materials present in the polyol product. Given that the retention times for β-caryophyllene and 1-thioglycerol are so similar to one another, it is unclear which of these two starting materials was left unreacted in the polyol product, BC-TG-ME. It can be seen from the peak at approximately

42 min retention time which appears in both the 2-mercaptoethanol and the BC-TG-ME curve, that there is also a slight amount of 2-mercaptoethanol which was left unreacted in the product curve at the time the reaction was stopped. Overall, the contributions of unreacted starting material were very small in the product polyol BC-TG-ME. It can be seen from looking at the peaks in the BC-TG-ME curve from about 36.5 min to 38 min retention time that there is a distribution of molecular weight species which were formed in the product polyol. It appears that the middle and lower molecular weight species at 37.5 min and 38 min, respectively, were the major contributors to the polyol while the higher molecular weight species whose peak is at 36.5 min retention time was the minor contributor to the polyol product.

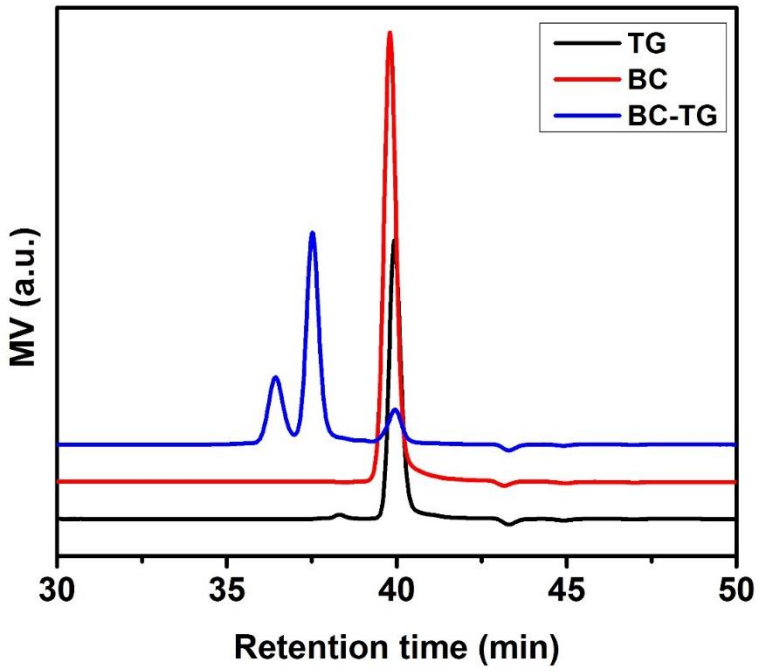

Figure 3.3: GPC curve of the BC-TG polyol and its starting materials.

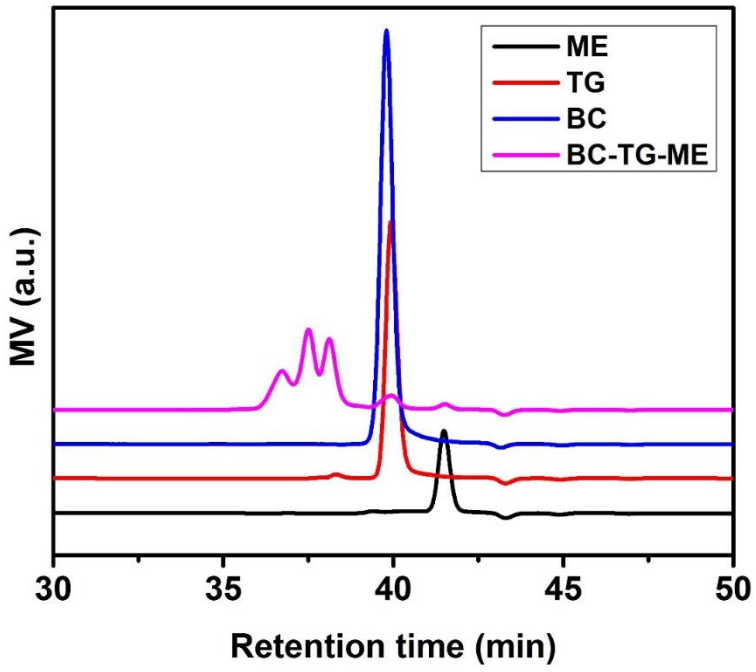

Figure 3.4: GPC curve of the BC-TG-ME polyol and its starting materials.

3.1.5. FT-Infrared Spectroscopy (FT-IR)

The infrared spectra of the starting materials and the synthesized polyols were recorded and analyzed. Figure 3.5 shows the FT-IR spectra of the polyol AP-TG and the starting materials from which it is derived. The appearance of a broad peak in the spectrum of polyol AP-TG around 3400 cm^{-1} indicates presence of an alcohol group which one would expect to see due to the reaction of double bond with 1-thioglycerol. There is a peak at approximately 2550 cm^{-1} in the spectrum for 1-thioglycerol which corresponds to the –S-H group. It can be observed in the spectrum for the product, AP-TG that this peak has disappeared indicating that the –S-H group is converted to –S-R by thiol-ene reaction. There is a peak around 3050 cm^{-1} in the α-phellandrene spectrum which is indicative of -C-H stretching from an alkene.

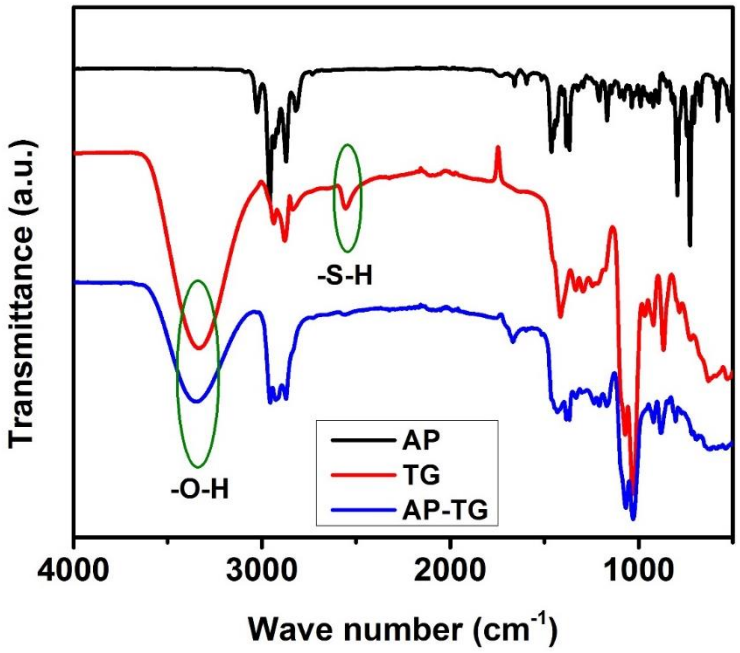

Figure 3.5: FT-IR of the polyol product AP-TG and its starting materials.

In the AP-TG product spectrum, it can be seen that the peak which was at 3050 cm^{-1} in the spectrum for α-phellandrene has shifted to 2950 cm^{-1}, indicating that alkene groups have reacted with 1-thioglycerol. These observations suggest that the reaction of thiol with alkene occurred.

The FT-IR spectra of polyol AP-ME-TG and its starting materials are shown in Figure 3.6. As seen in the spectra for both 1-thioglycerol and 2-mercaptoethanol, there is a peak around 2550 cm^{-1} which corresponds to the thiol groups in both of the starting materials. In the FT-IR spectrum for the polyol AP-ME-TG, the peak around 2550 cm^{-1} has disappeared which indicates that the thiol group has reacted with the double bond of the α-phellandrene. In the spectrum of α-phellandrene, a peak around 3050 cm^{-1} corresponds

to the presence of alkene groups. In the spectrum for AP-ME-TG, this peak has shifted to about 2950 cm^{-1} which indicates the alkene groups present in α-phellandrene have reacted. These two pieces of information together allowed it to be determined that thiol reacted with alkene and that formation of the polyol product was accomplished.

Figure 3.7 shows the FT-IR spectra of polyol BC-TG and the starting materials from which it is synthesized. The peak around 2550 cm^{-1} observed in the spectrum for 1-thioglycerol corresponds to the thiol group. As seen in the spectrum for the polyol BC-TG, the peak at 2550 cm^{-1} has disappeared which indicates that –S-H group is reacted and converted to –S-R group. A peak around 3000 cm^{-1} corresponds to the C=C bond of the β-caryophyllene. In the spectrum for BC-TG, this peak has shifted to about 2950 cm^{-1} which indicates the alkene groups present within the β-caryophyllene have reacted.

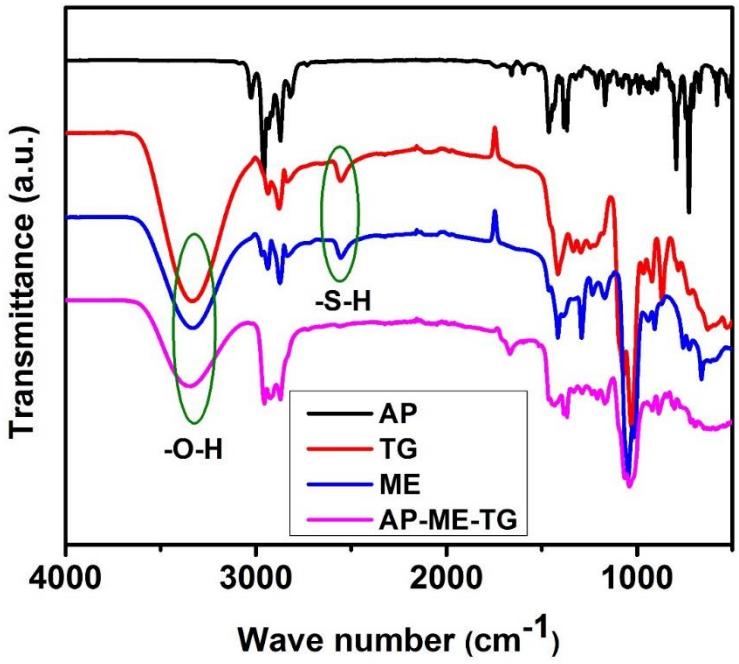

Figure 3.6: FT-IR of the polyol product AP-ME-TG and its starting materials.

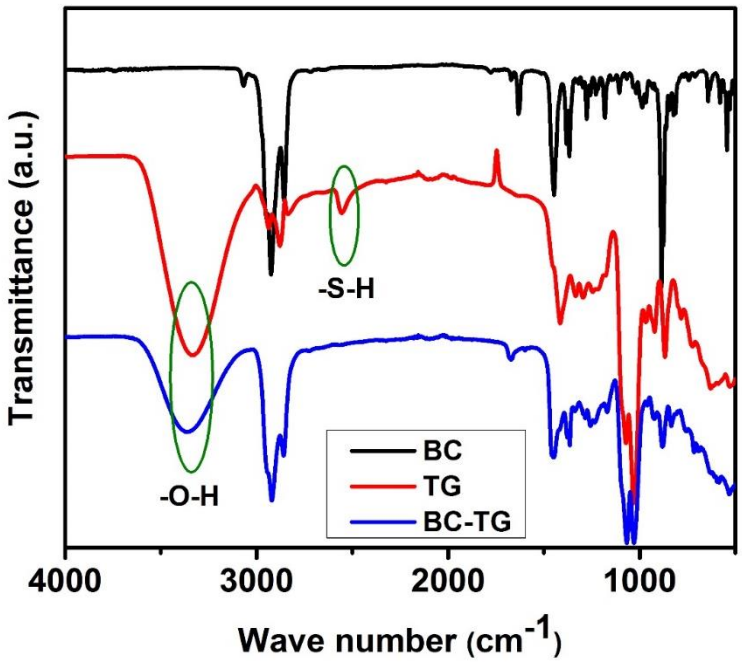

Figure 3.7: FT-IR of the polyol BC-TG and its starting materials.

The FT-IR spectra of polyol product BC-TG-ME and the starting materials is shown in Figure 3.8. It can be seen in the spectra for both 1-thioglycerol and 2-mercaptoethanol that there is a peak around 2550 cm^{-1} which corresponds to their thiol groups. As observed in the spectrum for the polyol BC-TG-ME, this peak has disappeared which indicates that the thiol group has reacted. In the spectrum of β-caryophyllene, a peak around 3000 cm^{-1} corresponds to the presence of an alkene group. In the spectrum for BC-TG-ME, one can see that this peak has shifted to about 2950 cm^{-1} which indicates the alkene groups present within β-caryophyllene have reacted. This indicates that the thiol-ene reaction did occur.

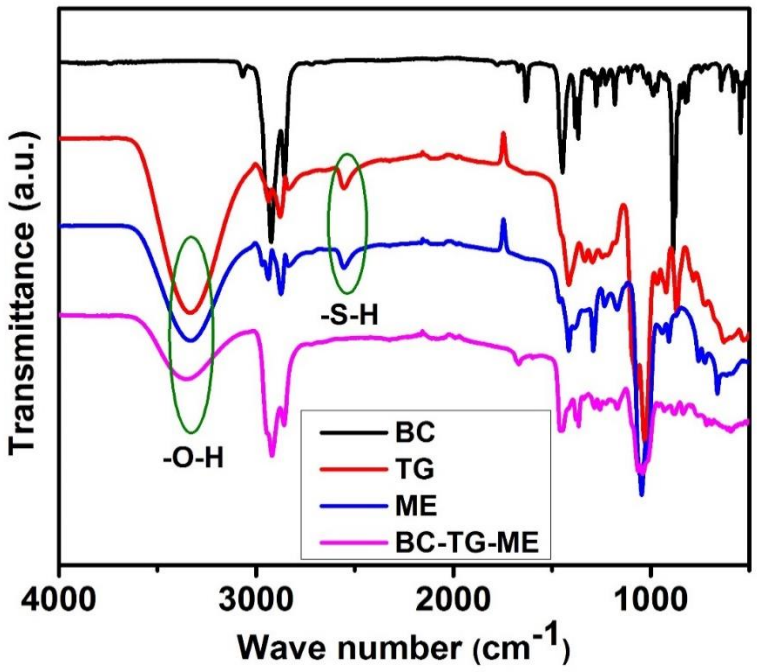

Figure 3.8: FT-IR of polyol BC-TG-ME and its starting materials

3.2. Rigid Polyurethane Foam Data and Discussion

Herein is presented the property data for the polyurethane foams which were synthesized in 50/50 blends of bio-based polyols and commercial Jeffol SG-360, and foams which were synthesized from pure bio-based polyols. A polyurethane foam made strictly using Jeffol SG-360 polyol was also prepared as a reference. The properties of foam which were studied and the results for which are presented here and discussed are: closed cell content, apparent density, 10 % compression strength, cell morphology, thermal stability and glass transition temperature. Other foam properties such as mix time, cream time, tack-free time and rise time of each of the foams were recorded and discussed. These times were recorded while the foaming reactions were in progress.

3.2.1. Foaming Reaction Times

The characteristic times for the polyurethane foams are given in Table 3.2 and Table 3.3. Mix time was the time spent homogenizing the reaction mixtures via mechanical stirring after Rubinate M (isocyanate) was added to polyols in the presence of catalyst, surfactant and blowing agent. Every effort was made to mix all foams for the same duration of time (around 11 seconds); however, this was not possible due to the higher reactivity of some of the mixtures. Cream time was the time recorded at which the reaction mixture visibly changed over from a liquid to a solid phase which began to rise as the reaction progressed. The tack-free time was the time when foam changed from a sticky texture to a hard texture. The rise time was the time recorded at which a foam rise was visibly stopped.

Table 3.2: Reaction times recorded during the synthesis of polyurethane foams based on 50/50 blends by weight.

Foam	Mix Time (s)	Cream Time (s)	Rise Time (s)	Tack-Free Time (s)
Foam 1	12	13	44	33
Foam 2	11	13	49	39
Foam 3	10	11	45	35
Foam 4	9	10	48	36
Reference Foam	11	13	62	45

Table 3.3: Reaction times recorded during the synthesis of polyurethane foams based on 100% bio-based polyol by weight.

Foam	Mix Time (s)	Cream Time (s)	Rise Time (s)	Tack-Free Time (s)
Foam 5	11	12	42	33
Foam 6	10	11	47	60
Foam 7	10	11	40	31
Foam 8	6	7	35	27
Reference Foam	11	13	62	45

Some of the foams synthesized underwent reduced mixing time as can be seen from Table 3.2 and Table 3.3. This was due to higher reactivity of the polyols towards isocyanate. Primary hydroxyl groups are more reactive toward isocyanate than the secondary hydroxyl groups due to reduced steric hindrance. The results which showed reduced mix time and higher extent of rising in some foams are likely due to the increased presence of primary hydroxyl groups. The polyol mixtures which involved the presence of 2-mercaptoethanol tended to be more reactive toward isocyanate than those foams which involved polyols which were made entirely using 1-thioglycerol. This is a result that is not surprising as 2-mercaptoethanol has only a primary hydroxyl group while 1-thioglycerol has both a primary and a secondary hydroxyl group. Therefore, any foam mixture which contained both 2-mercaptoethanol and 1-thioglycerol, as opposed to

solely 1-thioglycerol, had an increased presence of primary hydroxyl groups which made the polyol mixture more reactive towards isocyanate.

Figures 3.9-3.11 shows the pictures of the polyurethane foams. The effect of increased reactivity described earlier due to a higher presence of primary hydroxyl groups in those foams which included BC-ME-TG or AP-ME-TG in their polyol composition is evident by looking at the pictures for Foams 2, 4, 6 and 8 and observing that these foams, which contained AP-ME-TG or BC-ME-TG, rose to higher elevations than all of the other foams. Note that all of these photos were taken at approximately the same distance from the subject.

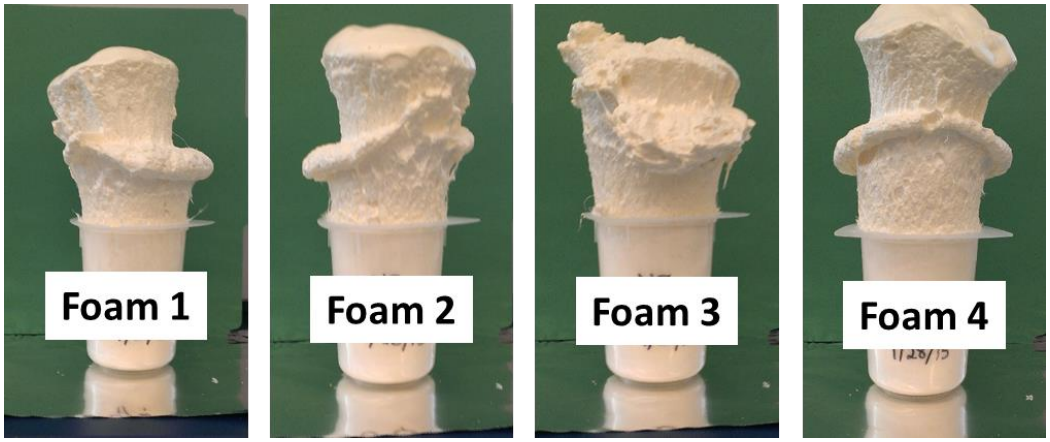

Figure 3.9: Photos of the prepared polyurethane foams using 50/50 Blends of polyols.

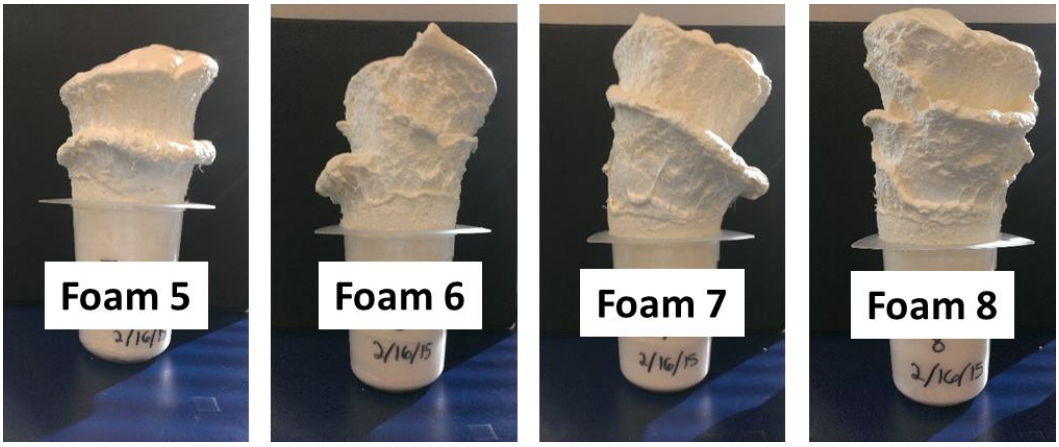

Figure 3.10: Photos of the prepared polyurethane foams using 100% synthesized polyols.

Figure 3.11: Photos of the prepared polyurethane foams using Jeffol 360.

3.2.2. Apparent Density

The apparent density for each foam was calculated for the top and middle portions of the foam in the direction of rise. The top portion's density was calculated from the rectangular prism shaped foam sample which served as the object of testing for the

compression strength of foams while the middle portion's density was calculated from the dimensions of the cylindrically shaped sample which was used to test closed cell content of the foams. The apparent densities of all foams were reported as the average of the densities which were calculated for the top and middle portions of each foam. The apparent density for each foam was reported in units of kg/m^3 (see Table 3.4 and Table 3.5). The acceptable range for apparent density of polyurethane rigid foams used for the purpose of thermal insulation by industry standards is between 30-40 kg/m^3. It can be seen from the Tables 3.4 and 3.5 that all of these foams fell within this range except for Foam 5 and Foam 8.

3.2.3. Closed Cell Content

Closed cell content is an important property of polyurethane rigid foams which are used for thermal insulation purposes. It is a measure of the amount of open cells which are present within the structure of a foam. Typically, for the purpose of thermal insulation, a highly desirable property of polyurethane rigid foam is a high percentage of closed cells in the structure (90% and above). The reason for this is that open cells allow air to pass through the foam structure. Closed cell content was studied and recorded for each of the foams using a HumiPyc pycnometer. The following equation was used to calculate percentage closed cell content (% CCC):

$$\% \text{ CCC} = \frac{\text{Vreal}}{\text{Vg}} \times 100\%$$

where, V_g is the geometrical volume of the foam sample and V_{real} is the actual volume occupied by the foam sample as calculated from the measurement of V_{VC} by the HumiPyc instrument. V_{real} was calculated using the following equation:

$$V_{real} = V_{chamber} - V_{VC}$$

Where, V_{VC} is the volume (found by testing) of empty space in the pynometer testing chamber that was not occupied by a foam sample and $V_{chamber}$ is the volume of the empty pycnometer testing chamber.

Table 3.4: Apparent density of polyurethane foams based on 50/50 blends.

Foam	Apparent Density (avg.) (kg/m^3)	Apparent Density (top) (kg/m^3)	Apparent Density (middle) (kg/m^3)
Foam 1	38.6	40.5	36.7
Foam 2	36.7	36.9	36.4
Foam 3	36.7	38.4	34.9
Foam 4	39.0	43.5	34.5
Reference Foam	37.5	36.9	38.0

Table 3.5: Apparent density of polyurethane foams based on 100 % synthesized Polyols.

Foam	Apparent Density (avg.) (kg/m^3)	Apparent Density (top) (kg/m^3)	Apparent Density (middle) (kg/m^3)
Foam 5	47.4	47.4	47.3
Foam 6	37.1	36.8	37.3
Foam 7	33.7	33.7	33.6
Foam 8	28.3	29.1	27.4
Reference Foam	37.5	36.9	38.0

The results for the closed cell content are given in Table 3.6. For all the tests performed on foam, $V_{chamber}$ was equal to 110.77 cm^3. The highest values of closed cell content (95%) were obtained for Foam 1, Foam 3 and Foam 4. These three foams were also the only foams which had a higher closed cell content than the Reference Foam. The closed cell content of all the other foams was above 90% which is in agreement with the standards which industry desires for polyurethane foams for thermal insulation applications. Overall, the 50/50 blend foams (Foams 1-4) performed better in the area of closed cell content than the foams which were derived from 100% polyols (Foams 5-8). Of the foams which were based on 100% bio-based polyols, Foam 6 (derived from BC-ME-TG) performed the best with closed cell content of 94% which is equal to that of the commercial Reference Foam. Overall, it was found that the foams based solely on the AP polyols (Foams 7 and 8) did not perform as well in the area of closed cell content as all

but one of the other foams studied. However, when the α-phellandrene polyols were blended with commercial Jeffol SG-360 (Foams 3 and 4), the closed cell content was improved. Foams based solely on β-caryophyllene polyols performed better than foams based solely on α-phellandrene polyols. However, when both sets of polyols are blended with Jeffol SG-360, the α-phellandrene set of polyols performed better than the set of β-caryophyllene polyols.

Table 3.6: Closed cell content for the polyurethane foams.

Foam	CCC (%)	V_{real} (cm^3)	V_g (cm^3)	V_{VC} (cm^3)
Foam 1	95	37.6314	39.56	73.0225
Foam 2	94	38.8702	41.25	71.7837
Foam 3	95	38.3830	40.37	72.2709
Foam 4	95	38.5671	40.71	72.0868
Foam 5	92	37.3913	40.57	73.3790
Foam 6	94	37.9130	40.23	72.8573
Foam 7	92	35.9477	38.89	74.8226
Foam 8	91	35.9320	39.57	74.8383
Reference Foam	94	38.4229	41.08	72.3474

3.2.4. Thermal Degradation Properties

Figure 3.12 shows the TGA curve for Foam 1 (derived from 50% BC-TG and 50% Jeffol SG-360 by weight). It was found that the onset degradation temperature for Foam 1 occurred at 244 °C. The material had further degradation peaks which occurred at 290°C, 327°C, 363°C and 489°C. These peaks correspond with the maxima which occur in the derivative plot (%/°C) curve which is shown in blue. According to this curve, the material degrades the most and at the fastest rate within the temperature range of 244-400°C. Overall, Foam 1 lost 87.5% of its weight by the end of the TGA run at 600 °C.

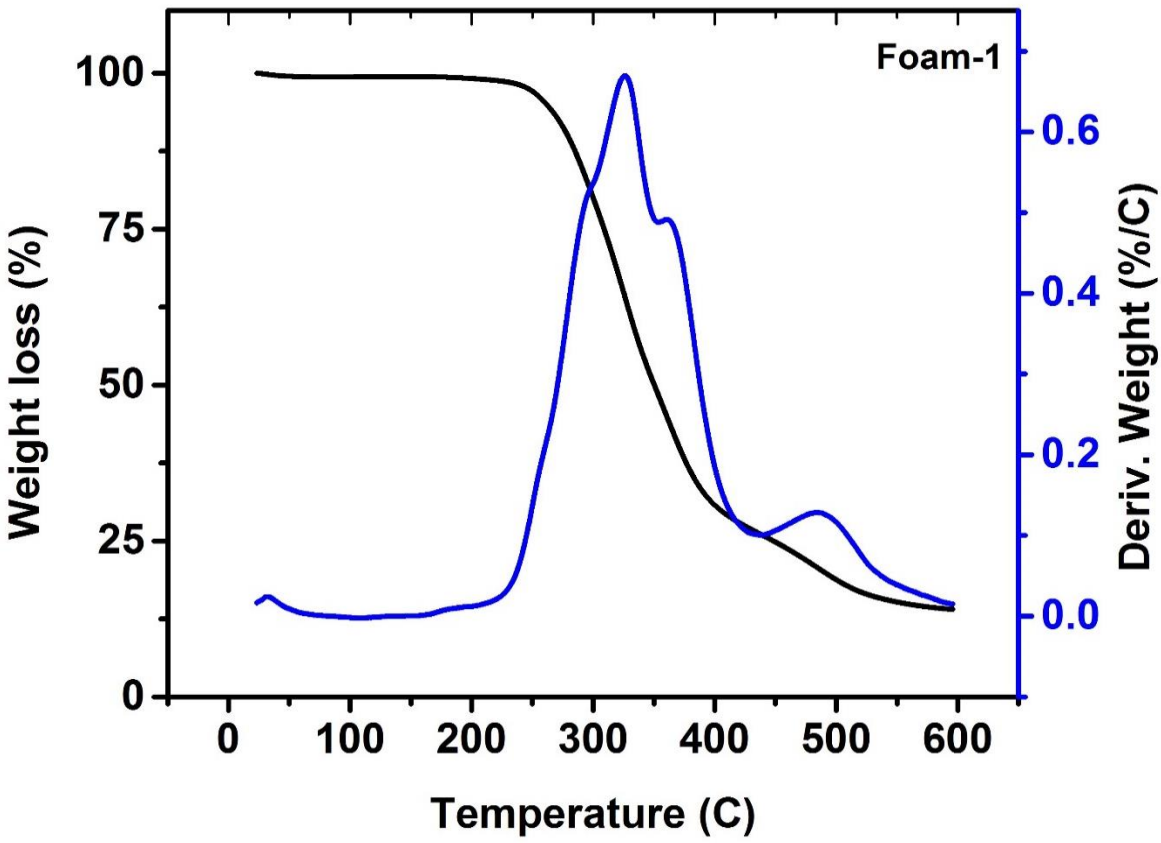

Figure 3.12: TGA curves for the Foam 1.

The TGA curves of Foam 2 are shown in Figure 3.13 which was derived from 50% BC-ME-TG and 50% Jeffol SG-360. As seen in the Figure 3.13, Foam 2 was thermally stable up to 237 °C which was its onset degradation temperature. The material had further thermal degradation peaks which occurred at 254 °C, 287 °C, 330 °C, 368 °C and 489 °C (shown by local maxima in the derivative plot). The foam degraded the most and at the fastest rate within the temperature range of 237-400 °C. The fastest rate of degradation was 0.65%/°C which occurred at 330°C. Foam 2 lost 87% of its weight when heated to 600 °C.

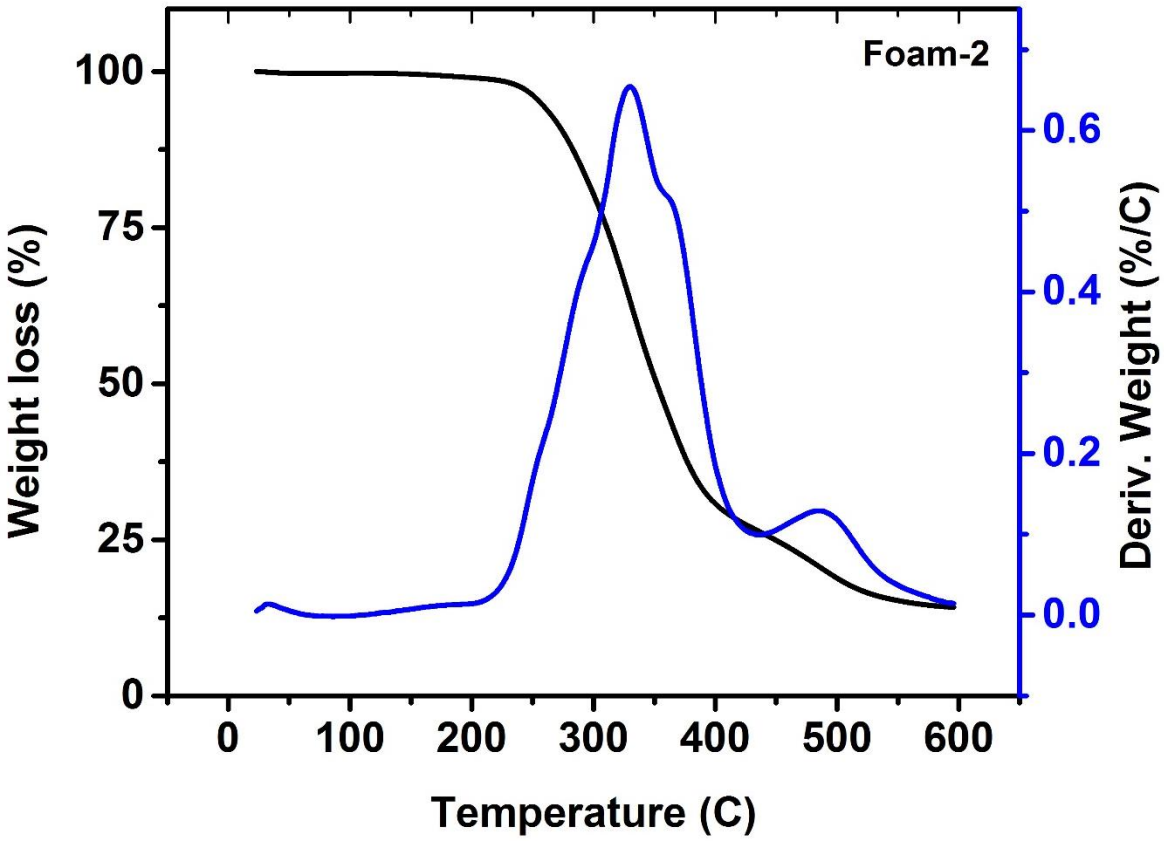

Figure 3.13: TGA curves of the Foam 2.

The thermal behavior of Foam 3 is shown in Figure 3.14. Foam 3 was prepared using 50% AP-TG and 50% Jeffol SG-360. As seen in the Figure 3.14, Foam 3 was thermally stable up to 238 °C. It is further evident from the TGA curves that Foam 3 has other degradation peaks at 259 °C, 290 °C, 328 °C, 372 °C and 487 °C, which can be seen as the maxima in the derivative plot. The material degraded the most and at the fastest rate within the temperature range of 238-400°C as can be seen from the height of the Derivative plot (%/°C). The foam degraded at its fastest rate of 0.67%/°C at 328 °C. Overall, Foam 3 lost 86% of its weight by the end of the TGA run.

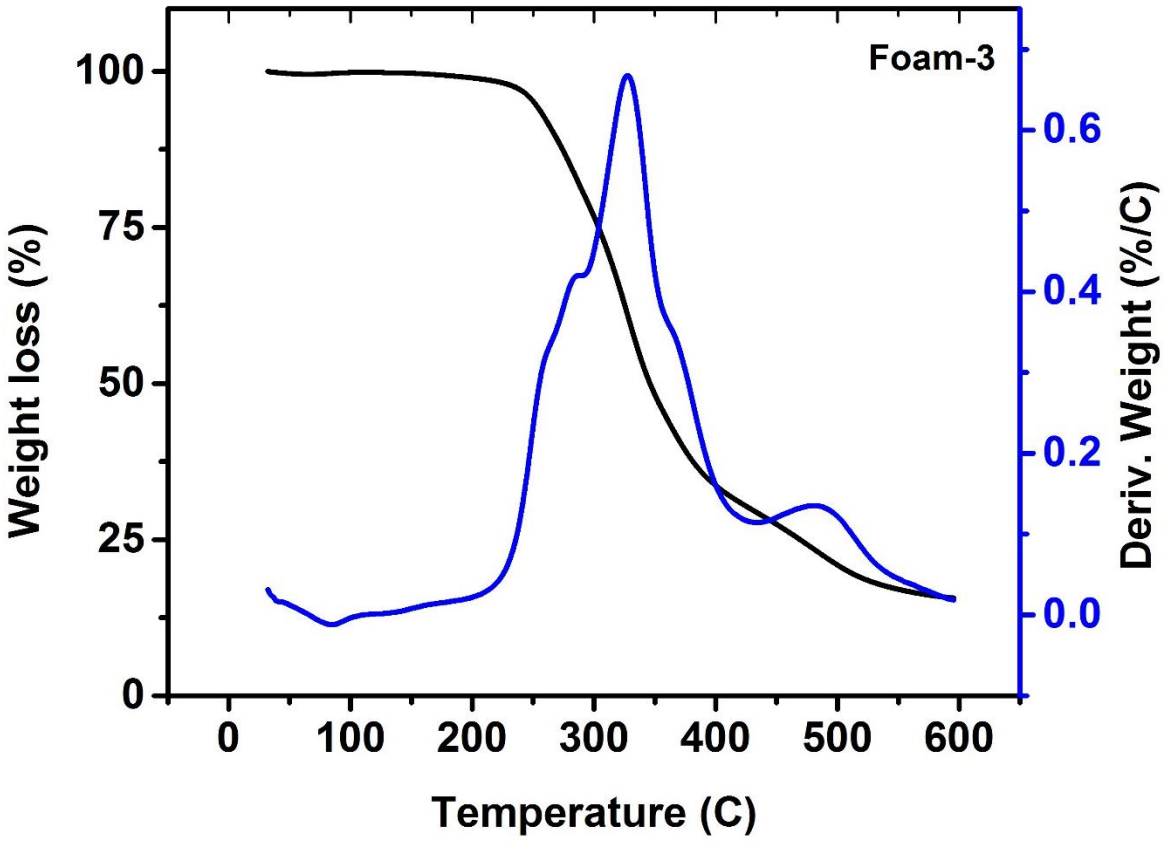

Figure 3.14: TGA curves for the Foam 3.

Figure 3.15 shows the TGA curve for Foam 4 (derived from 50% AP-ME-TG and 50% Jeffol SG-360). It was observed that Foam 4 was thermally stable up to 235 °C and after this it degraded quickly. Most of the transitions occurred at 257 °C, 290 °C, 326 °C, 372 °C and 488 °C. The material degraded the most and at the fastest rate within the temperature range of 235-400 °C as observed in the derivative plot. The fastest rate of degradation occurred at 326 °C with a rate of 0.68 % per °C. At the end of 600 °C, about 85% of the weight was lost.

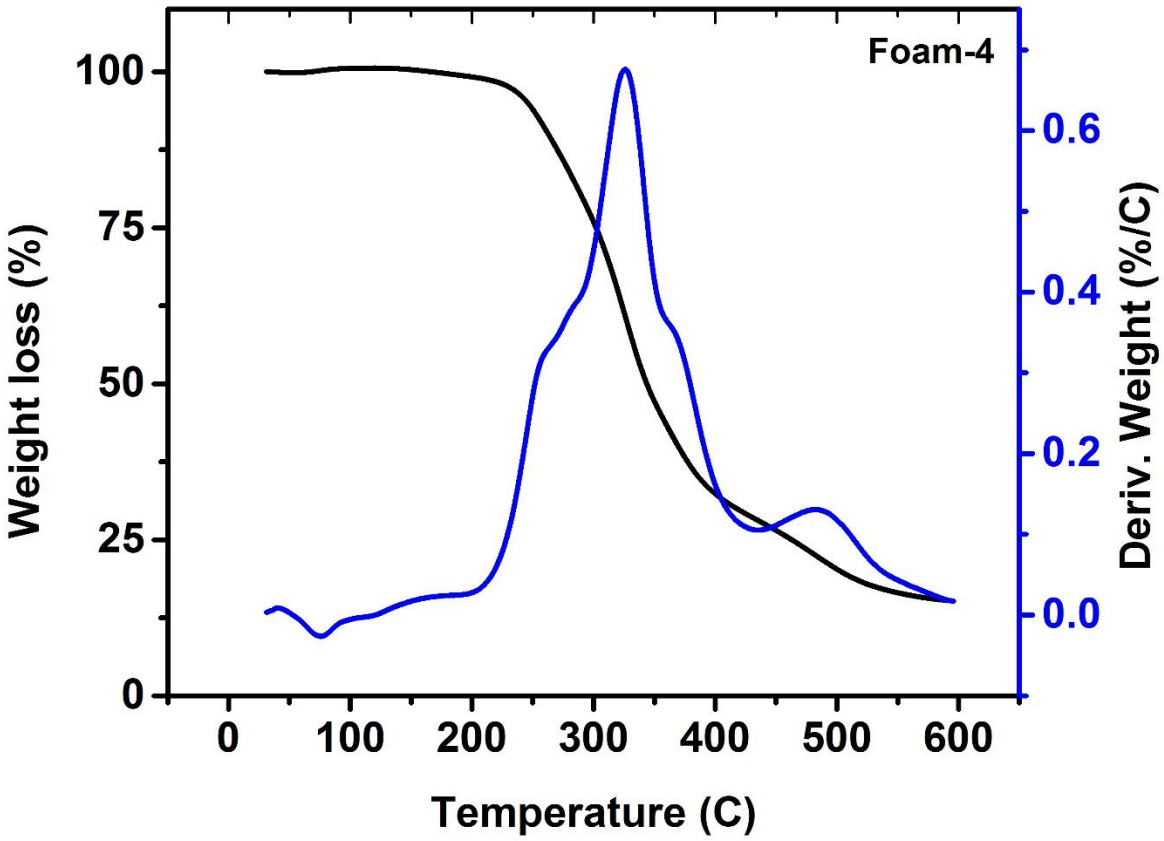

Figure 3.15: TGA curves for the Foam 4.

In Figure 3.16, the TGA curve depicting the thermal property of Foam 5 (derived from 100% BC-TG by weight) is shown. Foam 5 proved to be thermally stable up to 236 °C which was its onset degradation temperature. The material had degradation peaks which occurred at 252 °C, 286 °C, 332 °C and 483°C. The highest degree of degradation and the fastest rate of degradation occurred within the temperature range of 236-400 °C (indicated by the height of the blue curve within this region). The highest rate of degradation was 0.57% per °C which occurred at 286°C. Overall, Foam 5 lost 83% of its weight by the end of the TGA run.

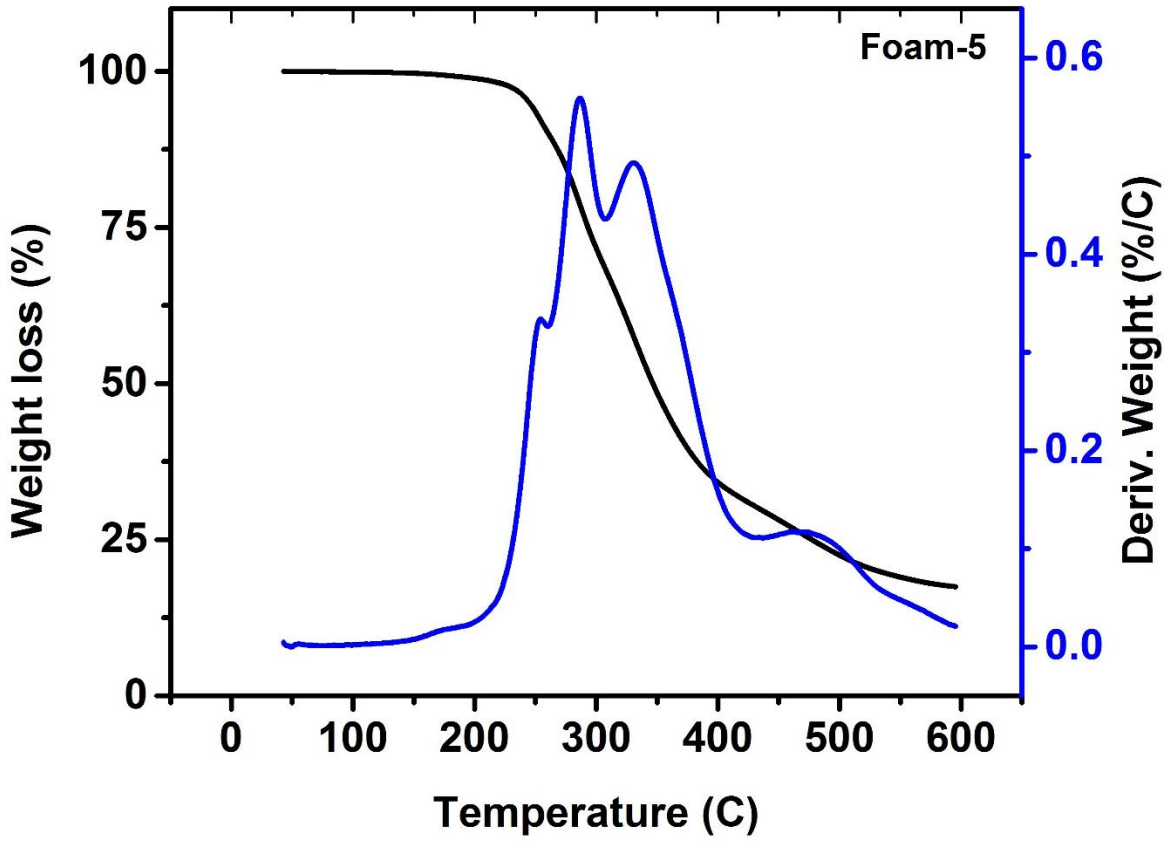

Figure 3.16: TGA curves of the Foam 5.

Figure 3.17 shows the TGA curve for Foam 6 which was prepared using 100 % BC-ME-TG. Foam 6 was found to be thermally stable up to 226 °C and after this the thermal degradation began. The foam also had several degradation peaks which occurred at 243 °C, 282 °C, 343 °C and 488 °C. Thermal degradation occurred the most and at the fastest rate within the temperature range of 226-400 °C as can be seen by observing the height of the blue curve within this region. The fastest rate of degradation for Foam 6 was 0.51% per °C which occurred at 282 °C. Overall, the foam lost 86 % of its initial weight by the end of the TGA run.

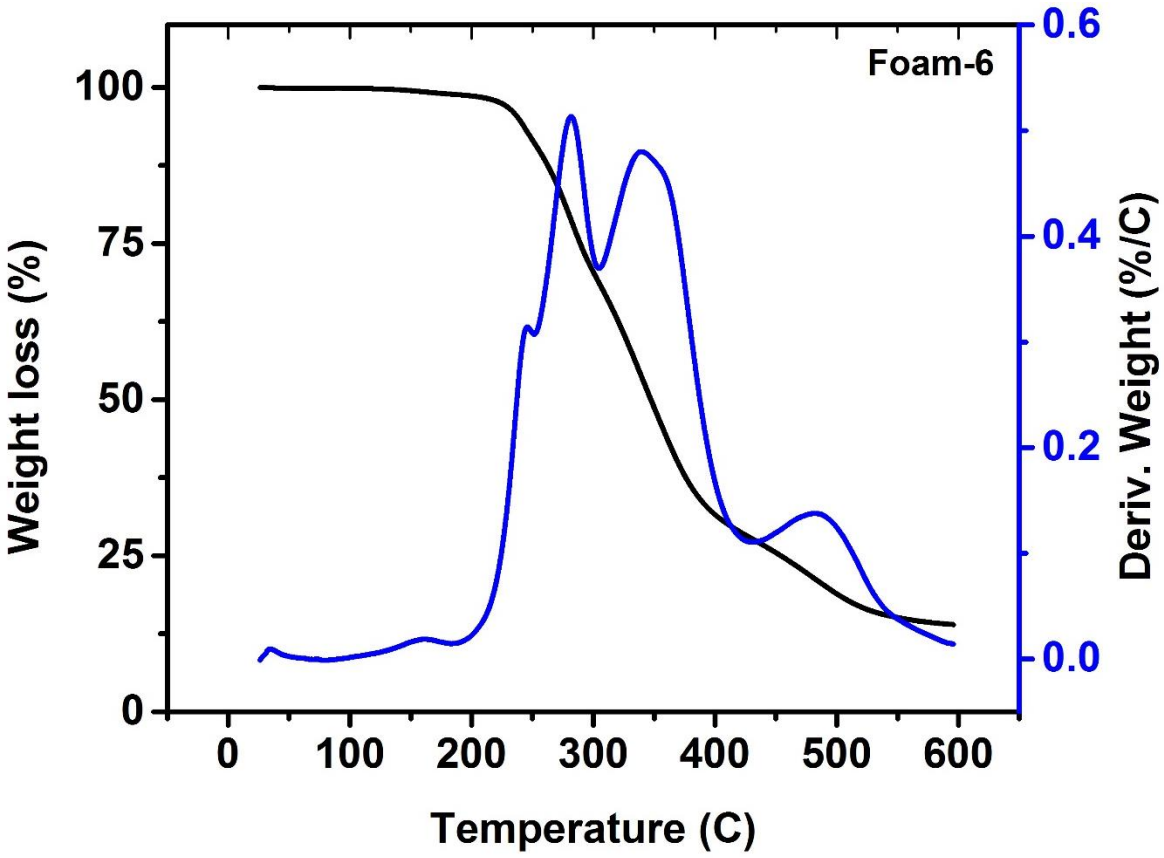

Figure 3.17: TGA curves for the Foam 6.

The TGA curves for Foam 7 are shown in Figure 3.18 which was derived from 100 % AP-TG by weight. The onset degradation temperature for Foam 7 occurred at 234 °C. The material also had thermal degradation peaks contained within its TGA curve which occurred at 255 °C, 275 °C, 323 °C and 483 °C. Foam 7 degraded the fastest and the most within the temperature range of 234-370 °C which is shown by the height of the derivative plot (%/°C) in this region. The highest rate of degradation was 0.64% per °C which occurred at 275°C. The Foam 7 lost 84 % of its initial weight by the end of the TGA run.

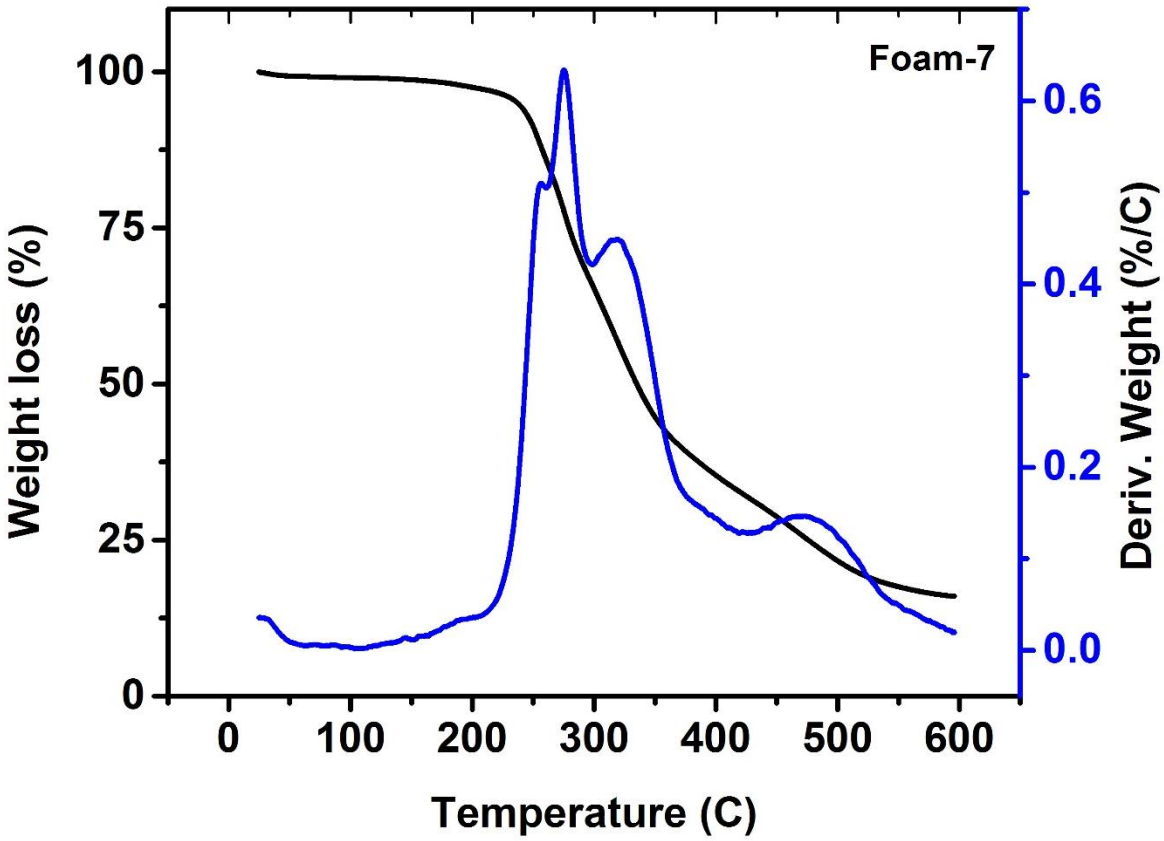

Figure 3.18: TGA curves for the Foam 7.

The TGA curve for Foam 8 which was derived from 100 % AP-ME-TG by weight is given in Figure 3.19. Foam 8 was determined to be thermally stable up to 228°C, and after this temperature thermal degradation began. The material also had degradation peaks in its curve which occurred at 251°C, 276°C, 323°C and 483°C. The foam degraded the fastest and the most within the temperature range of 228-400°C, as can be seen from the derivative plot in the Figure 3.19. The highest rate of degradation for Foam 8 was 0.54% per °C which occurred at 276°C. By the end of the TGA run, Foam 8 had lost about 85% of its initial weight.

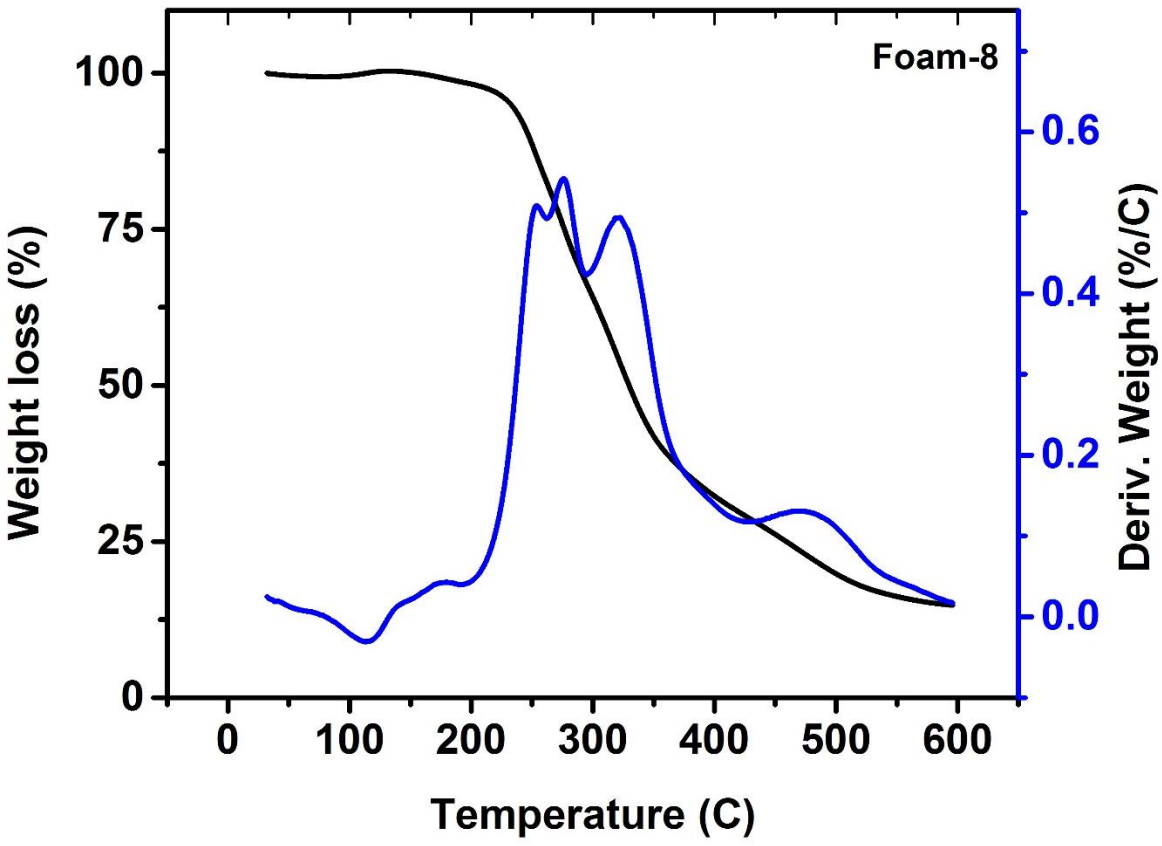

Figure 3.19: TGA curves for the Foam 8.

The TGA curve for the Reference Foam (derived from 100% Jeffol SG-360) is shown in Figure 3.20. The onset degradation temperature of the Reference Foam occurred at 266 °C. The material also had further thermal degradation peaks appear at 322 °C, 371 °C and 493 °C. The Reference Foam degraded the most and fastest within the temperature range of 266-420 °C. The highest rate of degradation was 1.1% per °C and it occurred at 322 °C. Overall, the foam lost 87.5% of its weight by the end of the TGA run.

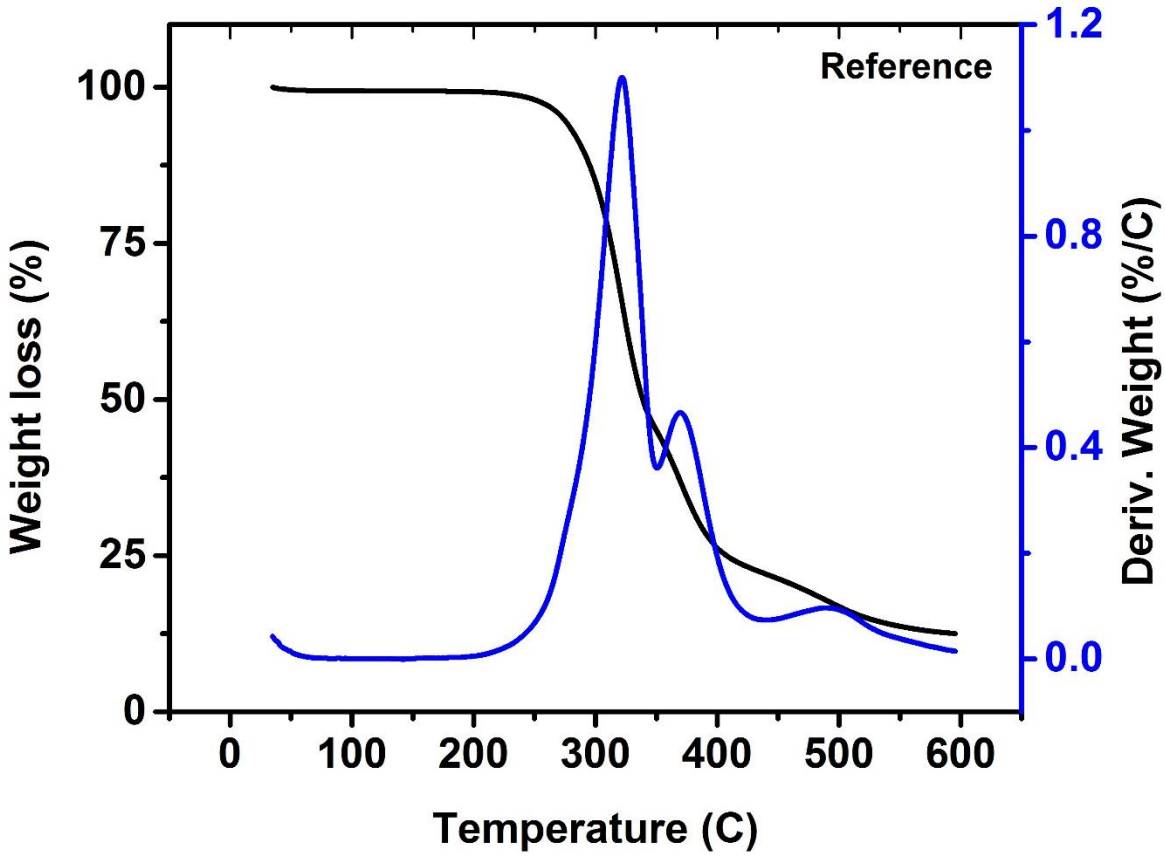

Figure 3.20: TGA curves for the Reference Foam.

The thermal degradation properties of all foams synthesized and studied in this research are presented in Table 3.7. Discussion on this table addresses the comparison between the thermal properties of 50/50 blend foams and 100% bio-based foams with the thermal properties of the Reference Foam.

Table 3.7: Comparison of the thermal degradation properties of all the prepared foams.

Foam	Onset Degradation Temperature (°C)	Maximum Rate of Degradation (%/°C)	Temperature of Maximum Rate of Degradation (°C)	Total Weight Loss (%)
1	244	0.68	327	87.5
2	237	0.65	330	87
3	238	0.67	328	86
4	235	0.68	326	85
5	236	0.57	286	83
6	226	0.51	282	86
7	234	0.64	275	84
8	228	0.54	276	85
Reference	266	1.1	322	87.5

Of the 100% bio-based polyurethane foams, it was determined that the β-caryophyllene-polyol-based foams (5 and 6) are more thermally stable than the α-phellandrene-polyol-based foams (7 and 8). This conclusion was drawn based on the fact

that the β-caryophyllene-based foams did not degrade as fast at their maximum rate of degradation as their counterparts of the α-phellandrene-based foams and that the temperature at which the maximum rate of degradation occurred was higher in the β-caryophyllene-based foams than the α-phellandrene-based foams. Foam 5 (based on 100% BC-TG) degraded at a maximum rate of 0.57% per °C which was less than the maximum rate of its α-phellandrene counterpart, Foam 7 (based on 100% AP-TG), which had a maximum rate of degradation of 0.64% per °C. Foam 5 also degraded fastest at a higher temperature than Foam 7: 286°C versus 275°C. Foam 6 (based on 100% BC-ME-TG) degraded at a maximum rate of 0.51% per °C which was less than the maximum rate of degradation for its α-phellandrene counterpart, Foam 8 (based on 100% AP-ME-TG), which degraded at maximum rate of 0.54% per °C. Foam 6 also degraded at its fastest rate at a higher temperature than Foam 8; 282°C versus 276°C. The onset degradation temperatures of the 100% β-caryophyllene-based foams and their counterparts of the 100% α-phellandrene-based foams were approximately the same; Foam 5 = 236°C versus Foam 7 = 234°C and Foam 6 = 226°C versus Foam 8 = 228°C.

It was found that when blended with Jeffol SG-360, the thermal property was better for Foams 1-4 than for their 100% bio-based counterparts (Foams 5-8), a conclusion which was drawn by looking at the onset degradation temperature and the temperature of maximum rate of degradation. It was also concluded that foams which had a higher content of 1-thioglycerol in their polyol makeup were considered to be more thermally stable than foams which had a bio-based polyol makeup which contained 2-mercaptoethanol. For instance, when comparing Foam 1 (based on 50% BC-TG) with

Foam 2 (based on 50% BC-ME-TG), Foam 1 has a higher onset degradation temperature (see Table 3.7). This same trend holds when comparing the onset degradation temperature of Foam 3 (based on 50% AP-TG) with Foam 4 (based on 50% AP-ME-TG), Foam 5 (based on 100% BC-TG) with Foam 6 (based on 100% BC-ME-TG) and Foam 7 (based on 100% AP-TG) with Foam 8 (based on 100% AP-ME-TG). It is hypothesized, though not confirmed, that the added thermal stability which results when a foam contains bio-based polyol, which solely contains 1-thioglycerol as a hydroxyl source versus foams which are made up of bio-based polyol, which contains 2-mercaptoethanol and 1-thioglycerol as a hydroxyl source, is due to the fact that more urethane linkages and a more interconnected polymer network is possible with 1-thioglycerol only because 1-thioglycerol has more hydroxyl groups than 2-mercaptoethanol in its structure. Total weight loss of all foams studied in this research were comparable.

Overall, Foam 1 was considered to perform the best among Foams 1-8 in the area of thermal stability based on the fact that its onset degradation temperature was the highest among Foams 1-8 and its temperature of maximum rate of degradation was third highest among Foams 1-8 with the property of onset degradation temperature being weighted more than all other thermal properties in importance. It was determined that none of the foams (1-8) performed as well as the Reference Foam (based on 100% Jeffol SG-360) in the area of thermal stability due to the fact that the onset degradation temperature was significantly higher (266°C) for the Reference Foam than it was for all of the other foams. The 50/50 blend polyurethane foams (1-4); however, all performed

better than the Reference Foam in the area of temperature of maximum rate of degradation.

3.2.5. Dynamic Mechanical Analysis (DMA)

Figure 3.21 depicts the DMA curves for Foam 1 which was derived from a polyol composition of 50% BC-TG and 50% Jeffol SG-360. The glass transition temperature for this foam as well as for all of the foams was determined from the maximum point in the tan delta curve shown in blue in DMA curves. The glass transition temperature for Foam 1 occurred at 209 °C at which point the tan delta curve reached its maximum value of approximately 0.51.

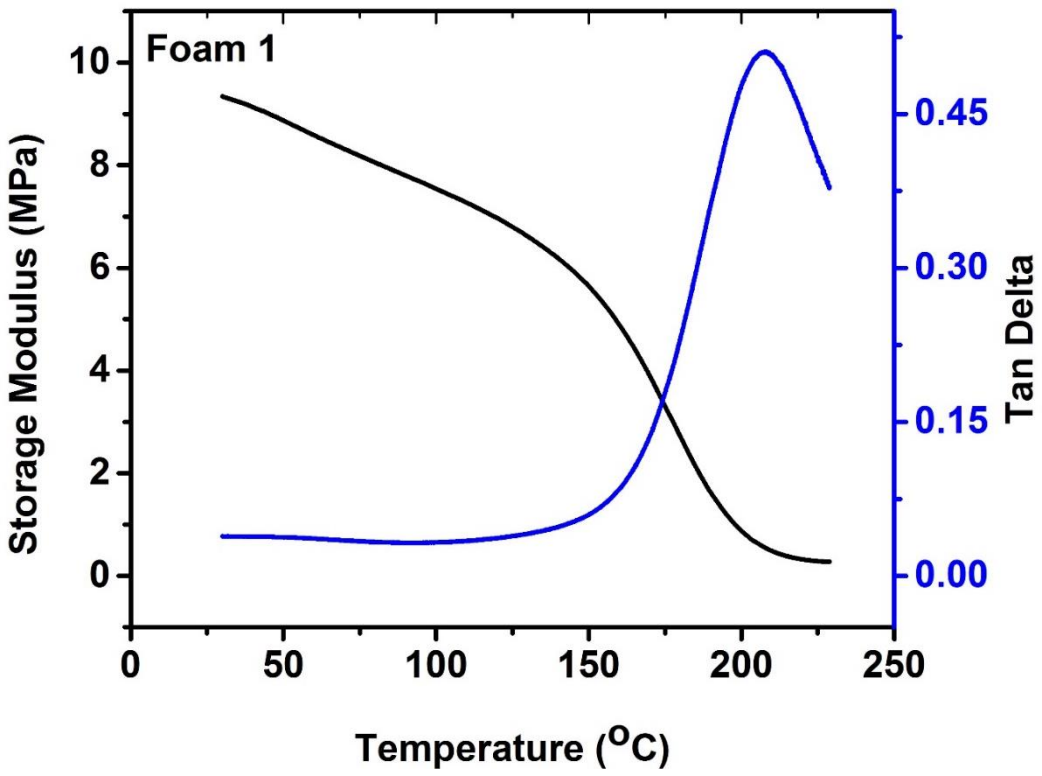

Figure 3.21: DMA curves for the Foam 1.

Figure 3.22 shows the variation of storage modulus and tan delta with temperature for the Foam 2. Foam 2 has a polyol composition which is 50% BC-ME-TG and 50% Jeffol SG-360. The glass transition temperature for this foam was found based on the maximum point of the tan delta curve which had a value of 0.60. The glass transition temperature for Foam 2 occurred at 189°C.

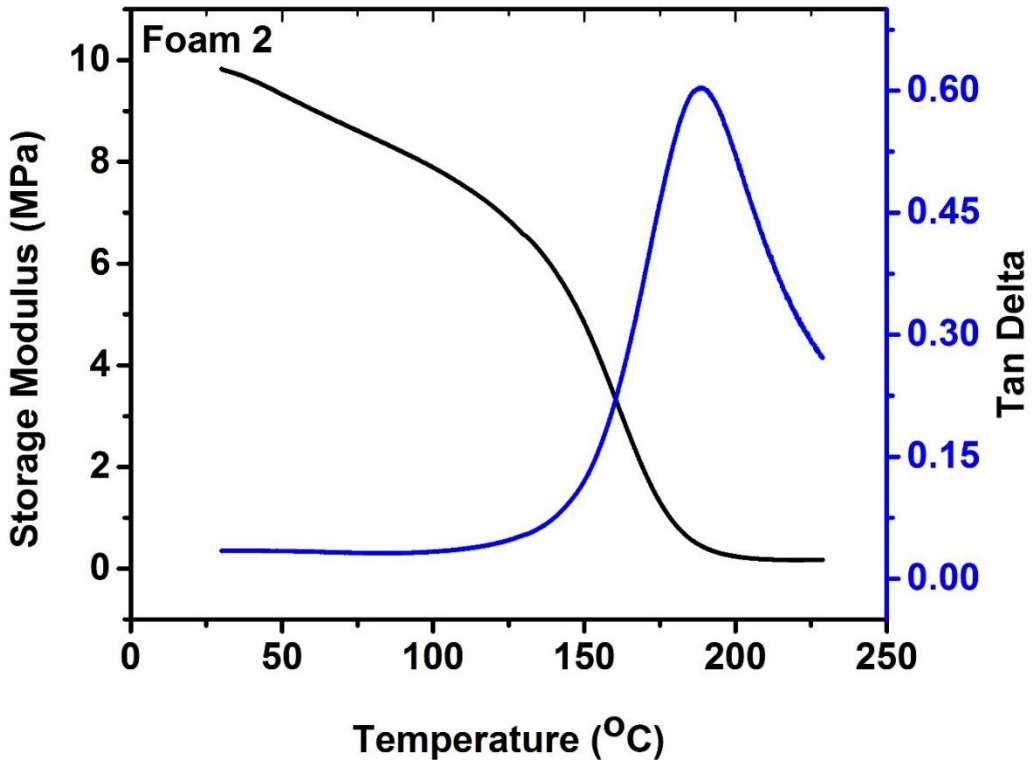

Figure 3.22: DMA curves for the Foam 2.

The DMA curves for Foam 3, which includes the storage modulus and tan delta plots, are shown in Figure 3.23. Foam 3 has a polyol composition which is 50% AP-TG and 50% Jeffol SG-360 by weight. The maximum point of the tan delta curve (shown in blue) has a value of approximately 0.43. The glass transition temperature for the foam which occurred at this value of the tan delta curve corresponds to a temperature of 218°C.

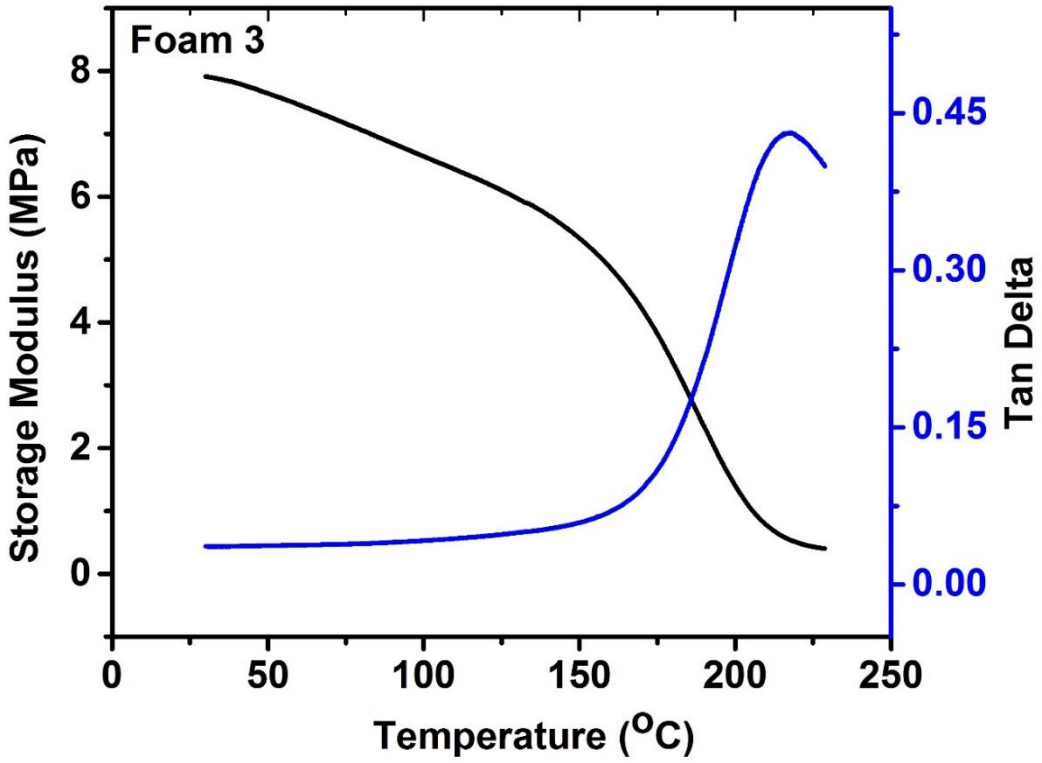

Figure 3.23: DMA curves for the Foam 3.

Portrayed in Figure 3.24 is the DMA curve for Foam 4 which shows data for the storage modulus and tan delta for the material. Foam 4 has a polyol composition of 50% AP-ME-TG and 50% Jeffol SG-360. The maximum point of the tan delta curve, which served as the point at which the glass transition of the material occurred, had a value of approximately 0.56. At this point, the glass transition temperature of the material occurred at a temperature of 196°C.

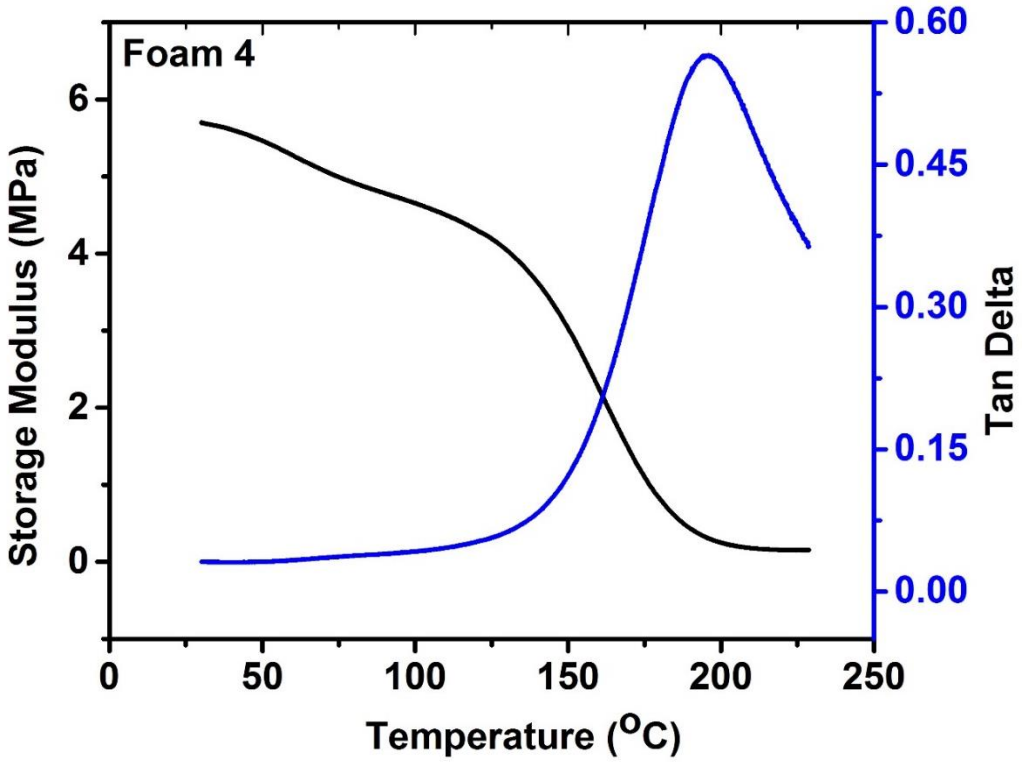

Figure 3.24: DMA curves for the Foam 4.

Pictured in Figure 3.25 is the DMA curve for Foam 5 which gives the storage modulus and tan delta data for the material. Foam 5 has a polyol composition of 100 % BC-TG. The maximum point in the tan delta curve shown in blue was 0.87. At this point, the glass transition of the foam occurred at a temperature of 201 °C.

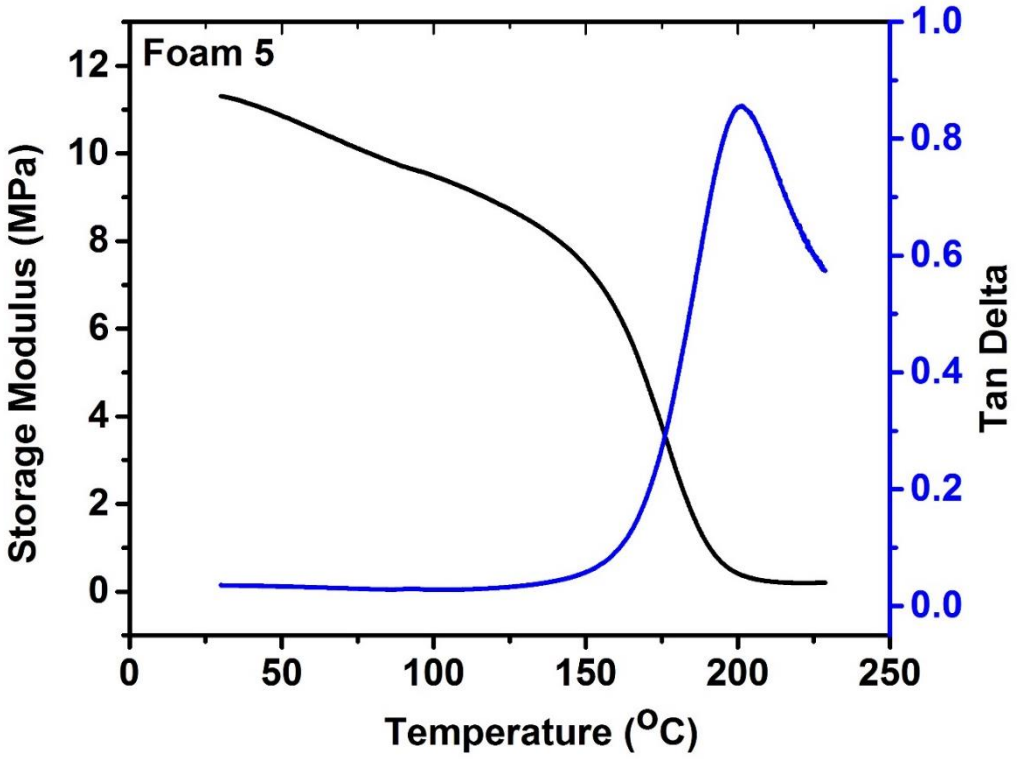

Figure 3.25: DMA curves for the Foam 5.

Figure 3.26 shows the DMA plots for Foam 6 which include the variation of storage modulus and tan delta with temperature. Foam 6 has a polyol composition by weight which is 100 % BC-ME-TG. The maximum point of the tan delta curve was 0.95. This point served as the point where the glass transition temperature of the material occurred. The value of the glass transition temperature for Foam 6 was observed to be 183°C.

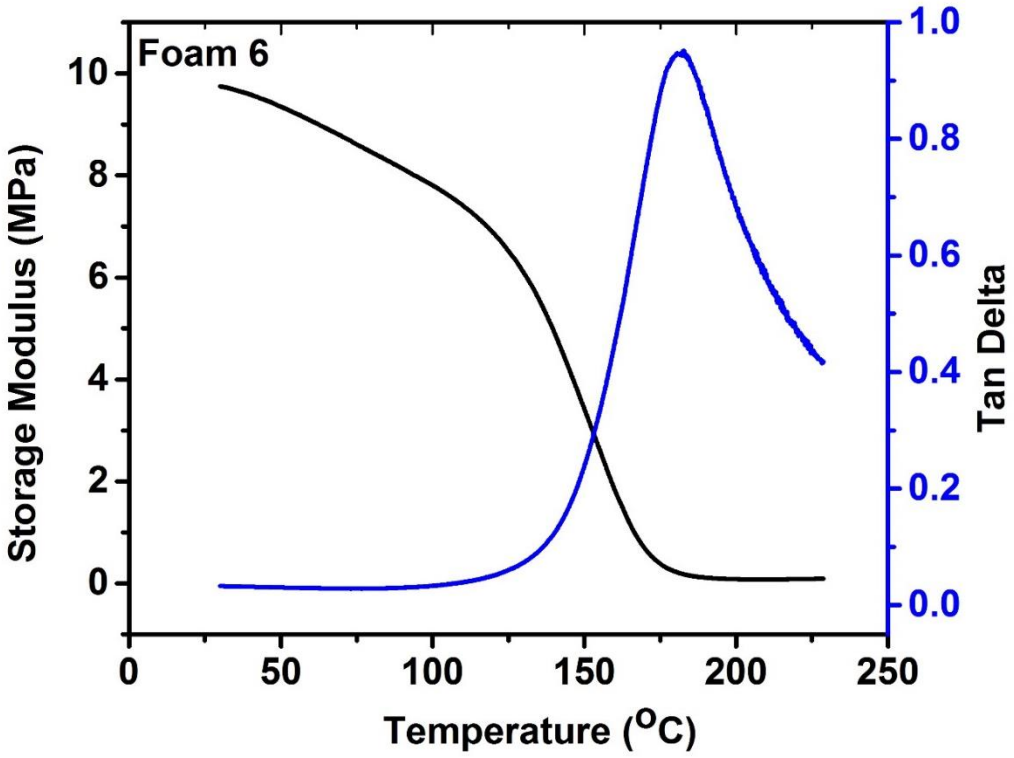

Figure 3.26: DMA curves for the Foam 6.

Figure 3.27 show the plots of the DMA data for Foam 7. Foam 7 was prepared using α-phellandrene and 1-thioglycerol. The maximum point of the tan delta curve was 0.56. This point served as the point where the glass transition temperature of the material occurred. The observed value of the glass transition temperature for Foam 7 was 229 °C.

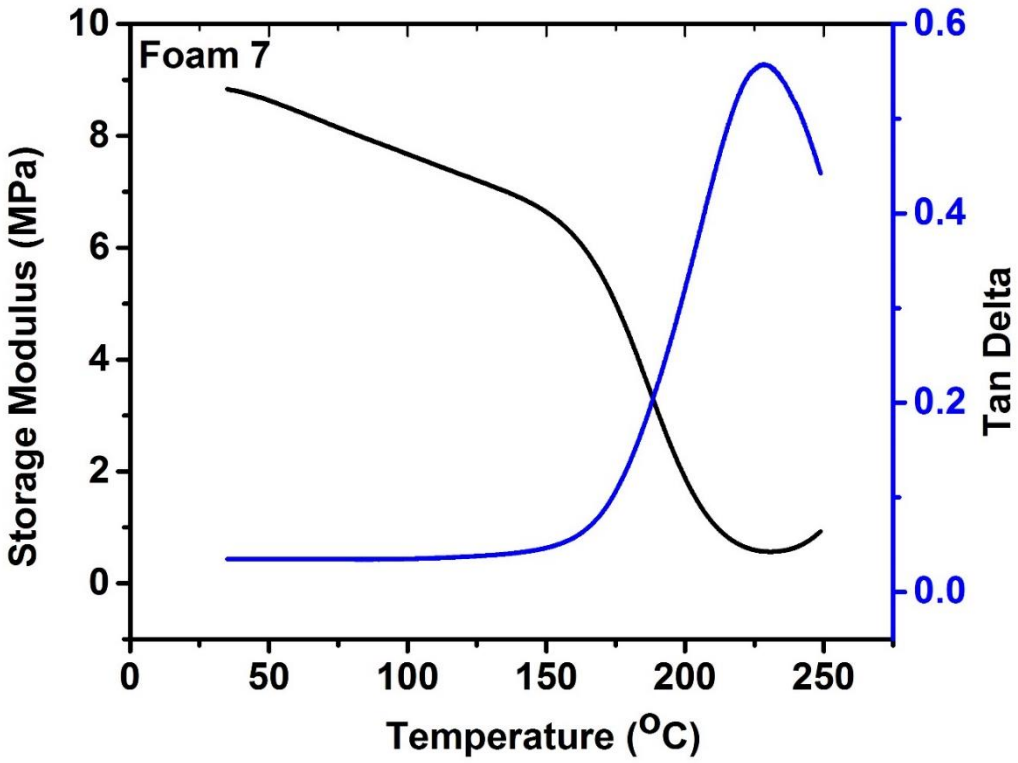

Figure 3.27: DMA curves for the Foam 7.

The DMA curves for Foam 8 is shown in Figure 3.28. Foam 8 has a polyol composition of 100% AP-ME-TG by weight. The maximum point of the tan delta curve, which served as the point at which the glass transition of the material occurred, had a value of approximately 0.74. At this point, the glass transition temperature of the material occurred at a temperature of 205°C.

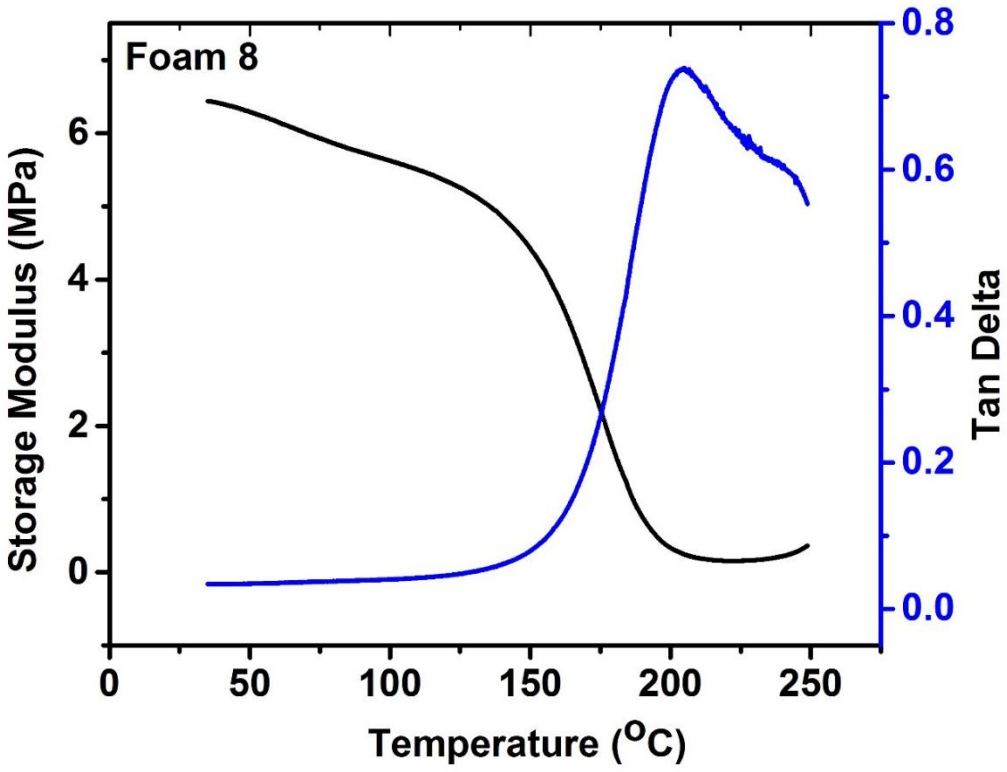

Figure 3.28: DMA curves for the Foam 8.

In Figure 3.29, the DMA curve for the industrial Reference Foam is shown. The Reference Foam had a polyol composition which was 100% Jeffol SG-360 by weight. Looking at the tan delta curve (shown in blue), it can be seen that the maximum point

occurs at approximately 0.45. At this point, the glass transition temperature for the Reference Foam was determined to be 183°C. Shown below in Table 3.8 are the glass transition temperatures for all foams which were synthesized and studied in this research. Discussion of the glass transition temperatures of the materials is given below as well.

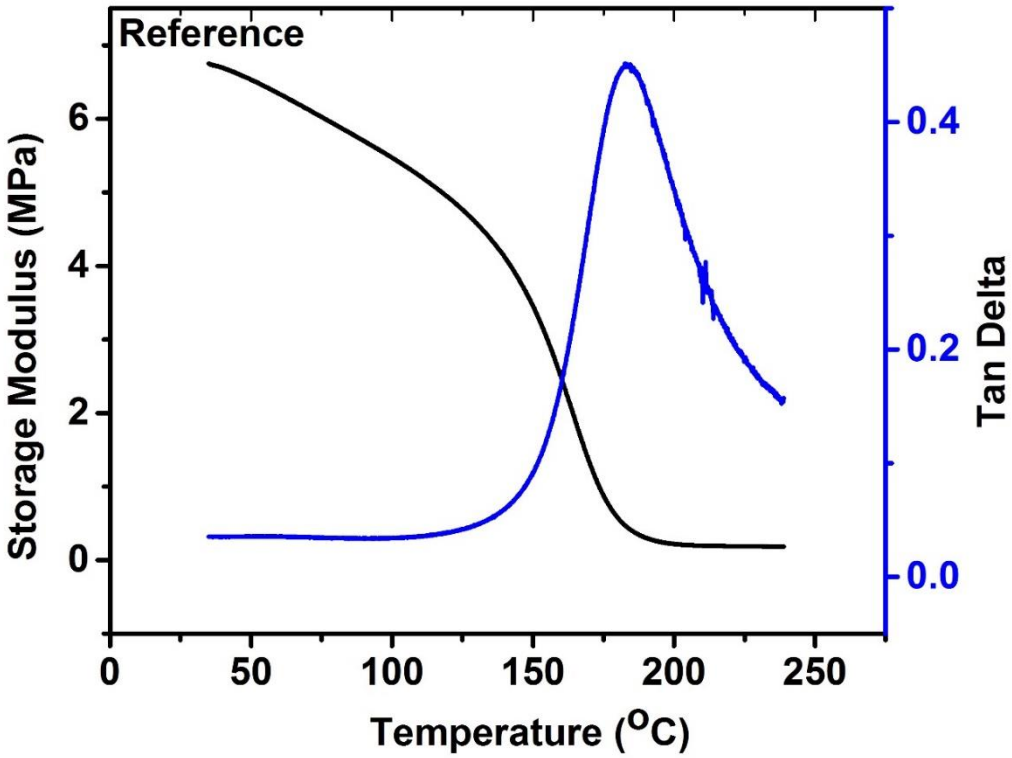

Figure 3.29: DMA curves for the Reference Foam.

Table 3.8: Comparison of the glass transition temperatures of all the foams.

Foam	Glass Transition Temperature (°C)
1	209
2	189
3	218
4	196
5	201
6	183
7	229
8	205
Reference	183

It was found that the glass transition temperature (T_g) of the foams which contained only 1-thioglycerol in their bio-based polyol content was higher than T_g for foams which contained 2-mercaptoethanol and 1-thioglycerol in their bio-based polyol content. For instance, Foam 1 (50% BC-TG) had a higher T_g (209°C) than Foam 2 (50% BC-ME-TG) which was equal to 189°C. Foam 3 (50% AP-TG) had T_g of 218°C while Foam 4 (50% AP-ME-TG) had a T_g of 196°C. Also following this trend are: Foam 5 (100% BC-TG) (201°C) versus Foam 6 (100% BC-ME-TG) (183°C) and Foam 7 (100% AP-TG) (229°C) versus Foam 8 (100% AP-ME-TG) (205°C).

It is predicted, though not confirmed, that the higher glass transition temperature of foams with AP-TG or BC-TG in their polyol composition could be due to a few different reasons. It could be that in Foams 1, 3, 5 and 7 there is a higher degree of cross-linking in the polyurethane structure than in Foams 2, 4, 6 and 8 which could potentially restrict the ability of the polymer chains to slide past one another in the foams where more urethane linkages are possible due to the increased amount of hydroxyl groups which can form them. Another possibility is that there is an increased amount of hydrogen bonding which holds the polymer chains more tightly associated to one another in Foams 1, 3, 5 and 7 than in Foams 2, 4, 6 and 8 due to the increased amount of urethane linkages which can form in this series of foams due to the higher functionality of the polyols that make them up. It was determined that the T_g of 100% α-phellandrene-based foams (7 and 8) was higher than T_g for their β-caryophyllene-based foam counterparts (5 and 6). This result also proved to be the case within the series of foams which were made of 50% bio-based material (Foams 1-4). This result could be due to a higher degree of neat packing of the polymer chains in foams which contained α-phellandrene-based polyols over that of the foams which contained β-caryophyllene-based polyols. If this is the case it could be explained by the fact that in the α-phellandrene-based foams there are cyclohexane rings in the structure which are able to stack nicely on top of one another while in the β-caryophyllene-based foams an irregular ring structure is present which includes a four and a nine membered ring which is very difficult to pack and thus the polymer chains in the foams which are β-caryophyllene-polyol-based are perhaps not as closely associated with one another as in the foams which have α-phellandrene-based-polyol structures.

The difference in the degree that the polymer chains are associated with one another plays a large role in determining how easily they can slide past one another. All of the foams which were synthesized and studied in this research surpassed the Reference Foam in the area of glass transition temperature except for one (Foam 6). It was found that though the T_g property of all 100% bio-based foams was good, the T_g property could be improved in foams which contained β-caryophyllene polyols by blending them with Jeffol SG-360 reference as the blend counterpart of 100% BC foams had a higher T_g value than the 100% foams: Foam 1 = 209°C versus Foam 5 = 201°C, Foam 2 = 189°C versus Foam 6 = 183°C. It was found that the 100% α-phellandrene-polyol-based foams associated better with themselves than when they were blended with Jeffol SG-360 as Foams 7 and 8 had higher T_g than their blend counterparts Foams 3 and 4.

3.2.6. Mechanical Property

Pictured in Figure 3.30 is the % strain versus stress curve comparing the mechanical property of blend polyurethane Foams 1-4 with the Reference Foam derived from 100% Jeffol SG-360. In Figure 3.31, the mechanical property of 100% bio-based polyurethane Foams 5-8 is compared with the Reference Foam. The 10% compression strength of each of the foams was recorded and the results of which are shown in Table 3.9.

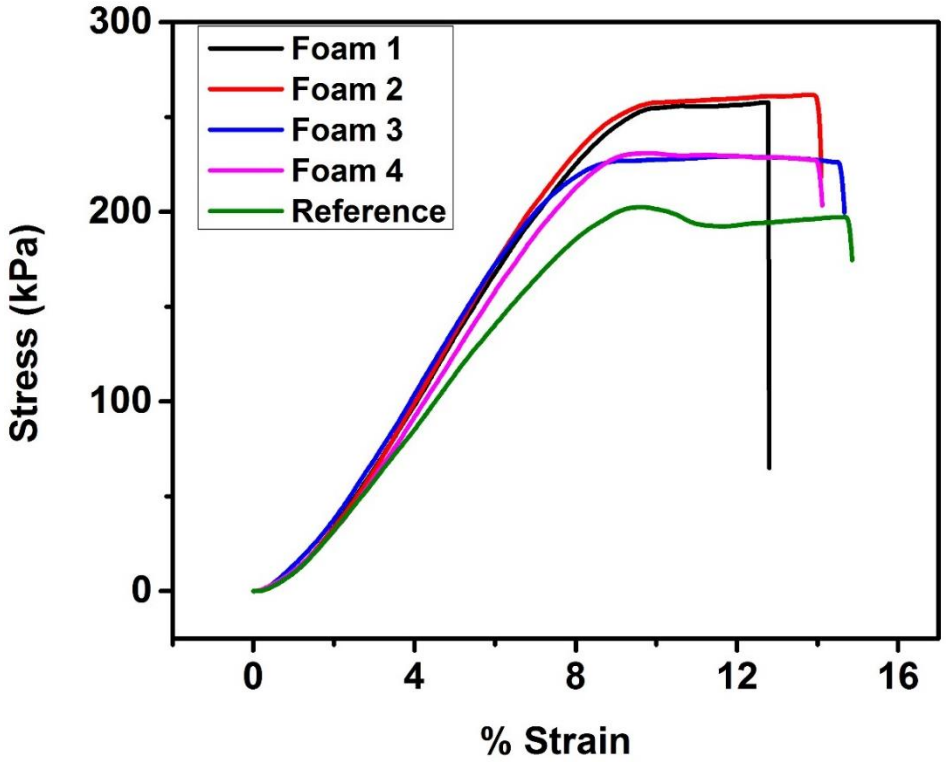

Figure 3.30: % Strain vs. stress curves for Foams 1-4 and Reference Foam.

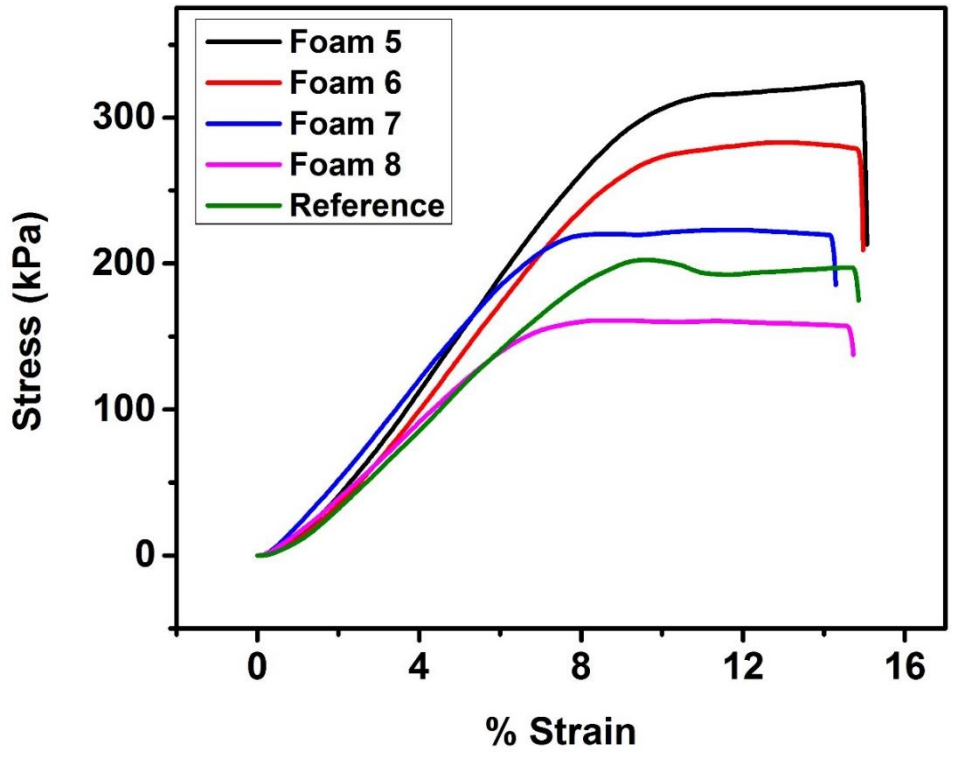

Figure 3.31: % Strain vs. stress curves for Foams 5-8 and Reference Foam.

Table 3.9: Compression strength at 10% strain for all the studied foams.

Foam	Compression Strength at 10% strain (kPa)
1	255
2	258
3	228
4	231
5	308
6	275
7	220
8	160
Reference	200

The compression strength at 10% strain for Foams 1-7 proved to be superior to the Reference Foam and, therefore, the mechanical property for these foams was better than the Reference Foam. Of all the foams, Foam 8 was the only foam which had a 10 % compression strength which was less than the Reference Foam. It was found that the mechanical property of foams made from β-caryophyllene polyols (both 50/50 blends and 100% bio based) was superior to the mechanical property of foams which were made from α-phellandrene polyols. This can be seen by comparing the 10% compression

strength of the 50/50 blends (Foams 1-4): Foam 1 (255 kPa) and Foam 2 (258 kPa) versus Foam 3 (228 kPa) and Foam 4 (231 kPa). The same trend also holds when comparing the 10% compression strength of the 100% bio-based polyurethane foams (5-8): Foam 5 (308 kPa) and Foam 6 (275 kPa) versus Foam 7 (220 kPa) and Foam 8 (160 kPa). The data for foams made from α-phellandrene polyols (Foams 3, 4, 7 and 8) shows that the mechanical property of 100% α-phellandrene-based foams could be improved by making a 50/50 blend with Jeffol SG-360. The 50/50 blend polyurethane foams which contained β-caryophyllene polyols had good mechanical property; however, by comparing the 10% compression strength values for Foams 1 and 2 with the values for Foams 5 and 6, it is evident that the β-caryophyllene-based foams have superior mechanical property when they contain 100% BC polyols in their composition. Of all of the foams which were synthesized and studied in this research, Foam 5 (based on 100% BC-TG) proved to have the most superior mechanical property with a 10% compression strength value of 308 kPa, which far surpassed all other foams. In the set of foams which were 100% bio-based polyurethanes, it was clear that foams made of polyols which contained only 1-thioglycerol as their hydroxyl group sources had greater mechanical property than foams which were made of polyols which contained half 1-thioglycerol and half 2-mercaptoethanol as their hydroxyl group sources. This was evident in both the β-caryophyllene based foams and the α-phellandrene-based foams as those which had all 1-thioglycerol (Foam 5 (100% BC-TG) and Foam 7 (100% AP-TG) had higher 10% compression strength values than those foams which had half 1-thioglycerol and half 2-mercaptoethanol (Foam 6 (100% BC-ME-TG) and Foam 8 (100% AP-ME-TG)). When each

of these foams were made into 50/50 blends with Jeffol SG-360, this trend was erased as all 50/50 blend polyurethane foams had comparable 10% compression strength values.

3.2.7. Microstructural Properties of the Foams

Figure 3.32 shows the surface morphology of Foam 1 (based on 50% BC-TG) using scanning electron microscopy (SEM). The cells in this foam are primarily of two different sizes with the exception of a few cells that are very small in length. It appears that the medium-sized cells and the larger cells tend to be in separate clusters. The cells are tightly compacted with one another such that there are very few open cells which agrees with the high closed cell content value for Foam 1.

The SEM image of Foam 2 (based on 50% BC-ME-TG) is shown in Figure 3.33. It appears that there are two primary sizes of cells within the structure: medium sized and small sized. When compared with the microstructure of Foam 1, it would seem that the structure of Foam 2 is less organized in terms of the arrangement of the cells. The size of the cells in Foam 2 are comparable to the sizes found in the structure of Foam 1. Like Foam 1, in the structure of Foam 2, there are very few open cells, which agrees with the value reported earlier for the closed cell content % of Foam 2. The pattern in the cell structure above is one in which medium-sized cells tend to be aggregated with one another with the occasional small cell filling in any gaps.

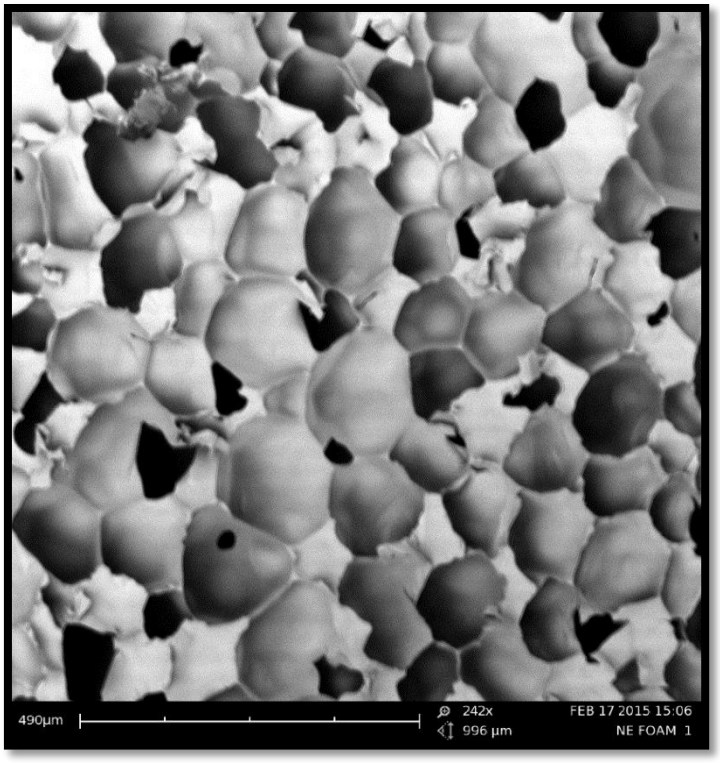

Figure 3.32: SEM image of Foam 1.

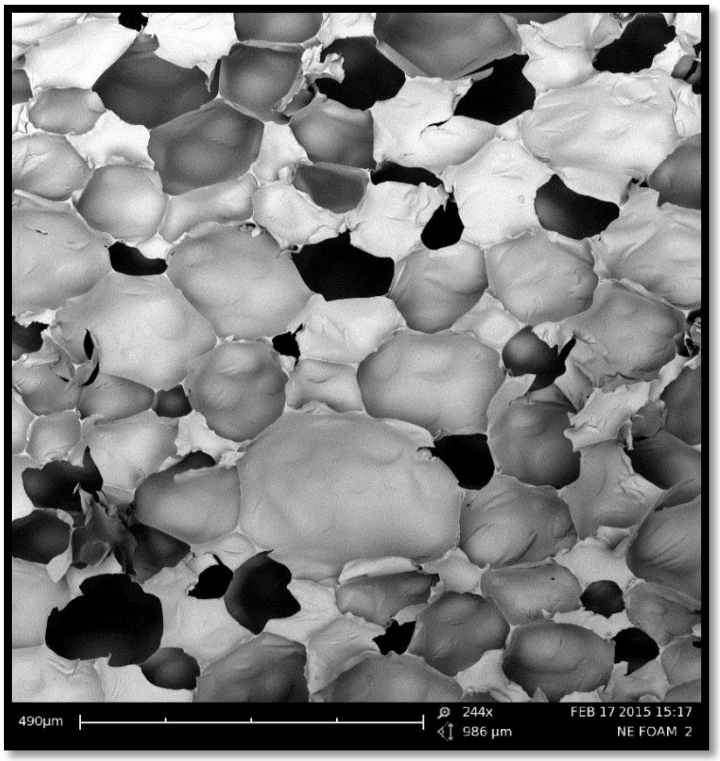

Figure 3.33: SEM image of Foam 2.

Figure 3.34 shows the SEM image of the surface microstructure of Foam 3 (based on 50% AP-TG). It appears that there are three primary sizes of cells within the surface structure: small, medium and semi-large sized. The arrangement of the cells is heterogeneous with no particular pattern. Holes in the cells are present to a moderate extent. It can be observed that the cell structure is very tight with very few open cells. This observation agrees with the result for the closed cell content of Foam 3 which was presented earlier. When compared with the cell structure of the β-caryophyllene-based blend polyurethanes (Foams 1 and 2) it is clear that the cell structure here for Foam 3 is less organized and more disperse. The medium-sized cells are the most prevalent type of cells which are found in the surface microstructure for Foam 3.

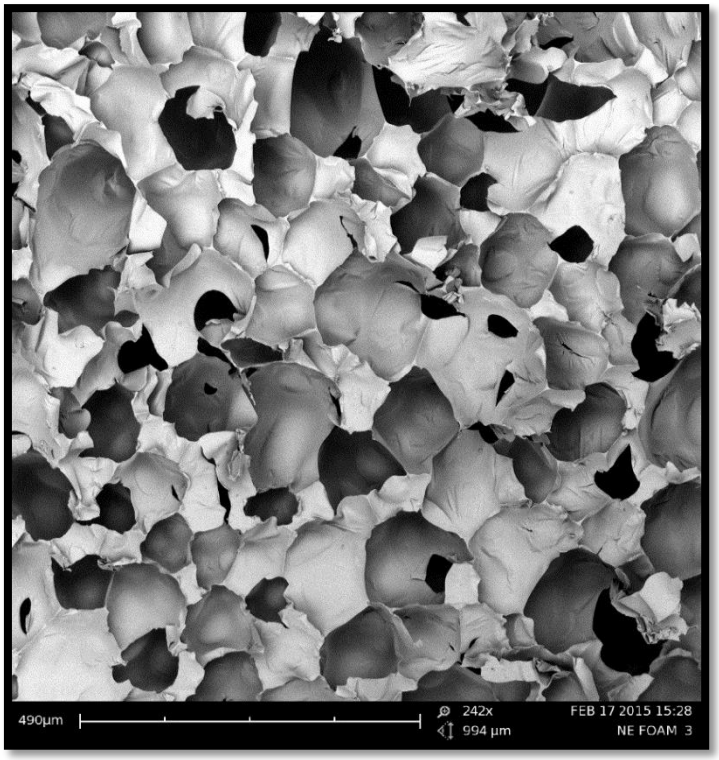

Figure 3.34: SEM image of Foam 3.

Figure 3.35 is the surface microstructure of Foam 4 (based on 50% AP-ME-TG) taken using SEM. Within the surface structure there are primarily two sizes of cells which make up most of the structure: medium and semi-large. In addition to this there are a few cells present which are small and a few which are large. The organization of the cells is more regular than for Foam 3 with semi-large cells being primarily grouped with one another and medium-sized cells dispersed throughout the photograph. Intercellular space is very small within the structure with very few open cells present.

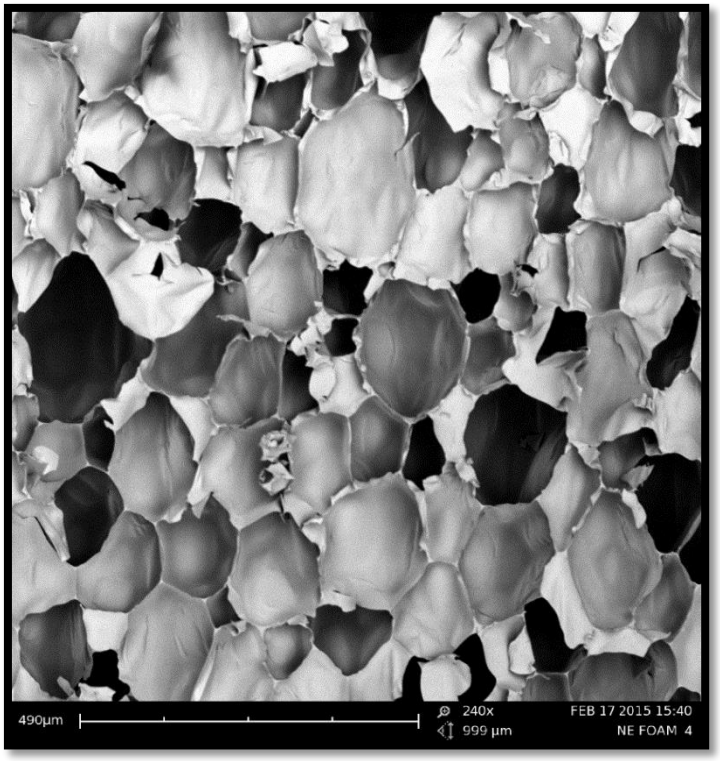

Figure 3.35: SEM image of Foam 4.

The SEM microstructure for Foam 5 (based on 100% BC-TG) is shown in Figure 3.36. By looking at the SEM image, it is evident that most of the cell sizes present within the microstructure are very small with the occasional presence of large cells and medium-sized cells incorporated in. This is a harsh contrast to the cell sizes which were present in Foam 1 when the BC-TG was blended with Jeffol SG-360. The organization of the structure of Foam 5 is very regular with the very small sized cells primarily associating with one another in a very tightly packed arrangement. As has been present in the structure of all polyurethane foams discussed up to this point, there are very few open cells present within the microstructure of Foam 5.

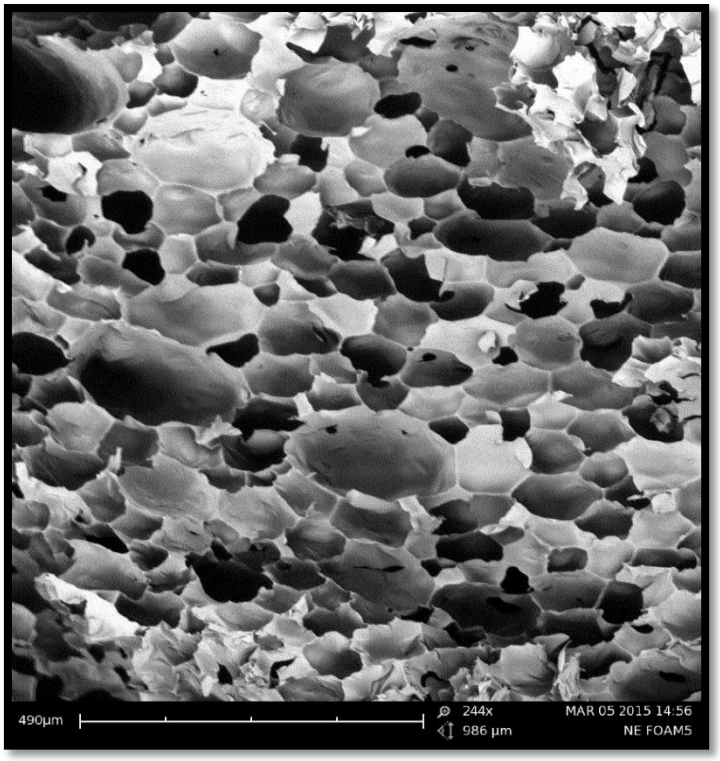

Figure 3.36: SEM image of the Foam 5.

In Figure 3.37, the surface microstructure of Foam 6 (based on 100% BC-ME-TG) is shown. Compared with the microstructure of Foam 5, Foam 6 has a less regular organization to its structure. There is also much difference in the size of the cells. In Foam 6, there are two primary sizes of the cells which are present: medium and semi-large. In addition to these sizes there are small and large sized cells which are present to a limited extent. It can be seen that the semi-large and the medium-sized cells tend to form their own clusters within the structure of Foam 6. Compared with its blend counterpart Foam 2, Foam 6 is less organized in the arrangement of its cells. The sizes of cells which are present in Foam 6 are comparable to the size of the cells found within its 50/50 blend counterpart, Foam 2.

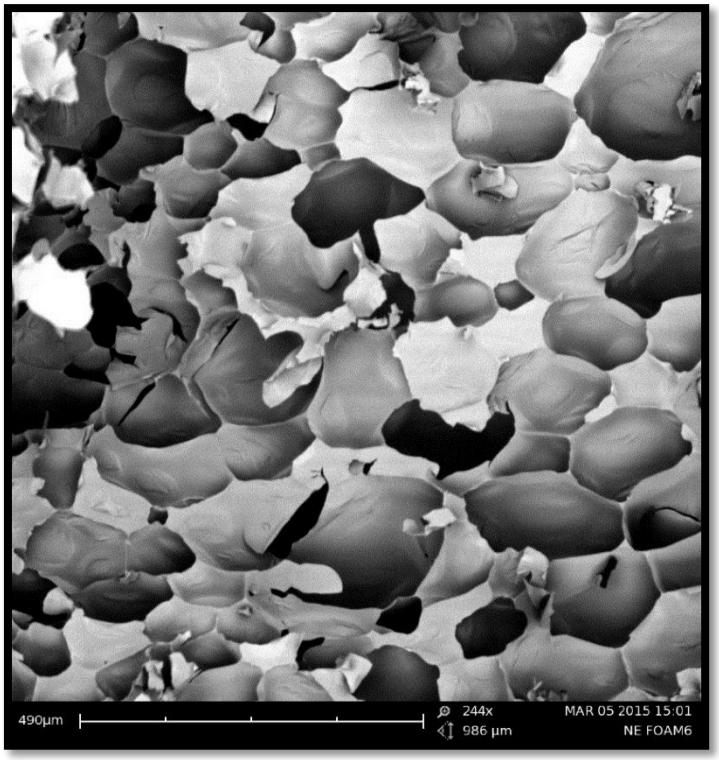

Figure 3.37: SEM image of the Foam 6.

Figure 3.38 shows the SEM microstructure of Foam 7 (based on 100% AP-TG). Within the structure, there are three primary cell sizes which are present: semi-large, medium and small. The organization of the cells is somewhat ordered. The medium and small-sized cells tend to form clusters of their own while the semi-large cells fill in the gaps which are present between these clusters. Compared with its 50/50 blend counterpart Foam 3, Foam 7 contains more of the larger cells and the order of its structure is less uniform than the structure which is present in Foam 3 in which there are primarily all medium-sized cells that are associated with one another.

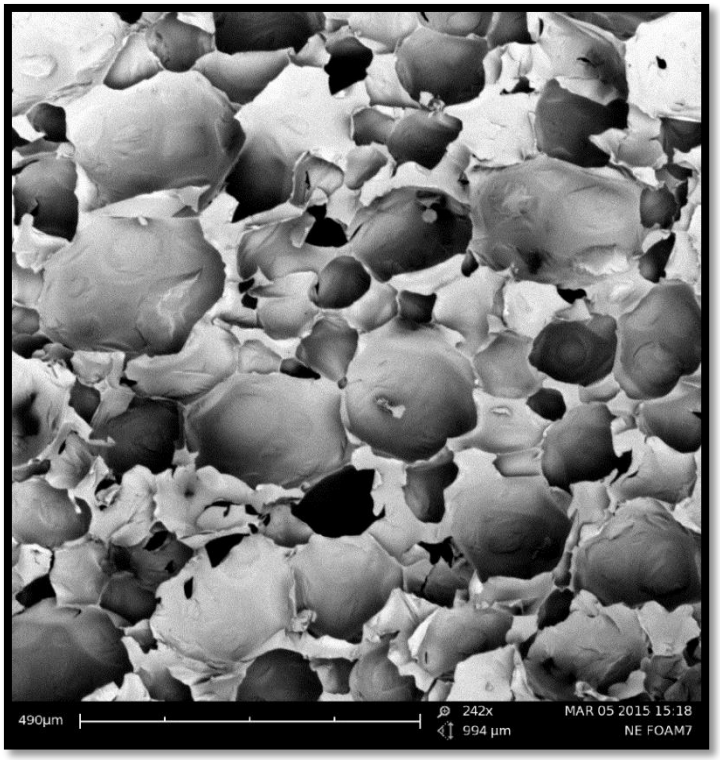

Figure 3.38: SEM image of the Foam 7.

Figure 3.39 shows the surface morphology of the Foam 8 (based on 100% AP-ME-TG). The cells present within the microstructure of Foam 8 are primarily of small, medium and semi-large sizes. The cells are neatly packed in arrangements in which semi-large and medium-sized cells form clusters with one another while the small-sized cells fill in the gaps between the bigger cells. The organization of the cells is uniform with very few open cells present within the microstructure. Compared with its 50/50 blend counterpart, Foam 4, Foam 8 has both similar cell sizes and overall arrangement of the cells.

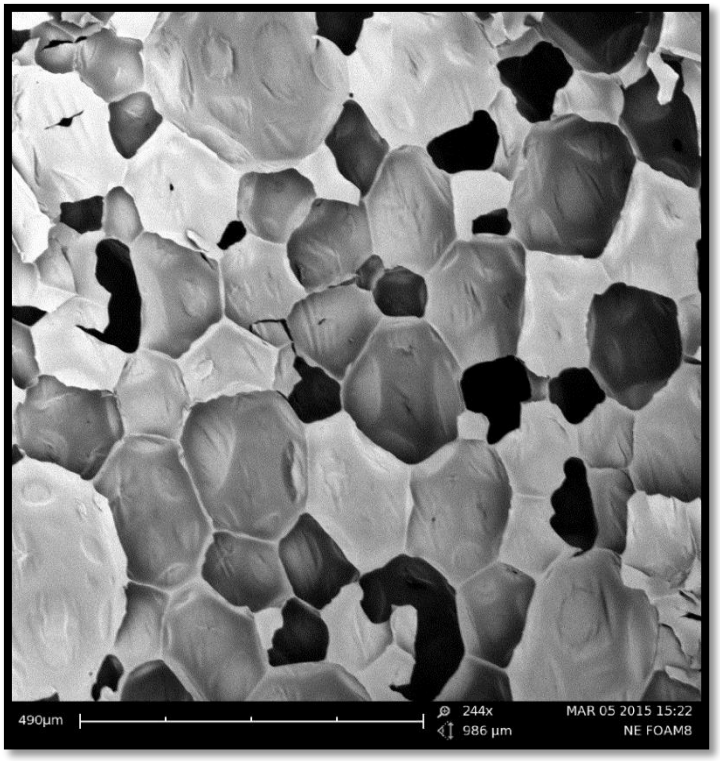

Figure 3.39: SEM image of the Foam 8.

Figure 3.40 shows the SEM microstructure of the Reference Foam (based on 100% Jeffol SG-360). The cells within the structure of the Reference Foam are primarily of three different sizes: medium, semi-large and large. There are also a few small sized cells which appear to a limited extent. When compared with all of the other foams which were synthesized and studied in this research, the Reference Foam had cellular sizes which were overall much larger than all of the other foams. The arrangement of the cells is tight and uniform with very few open cells present.

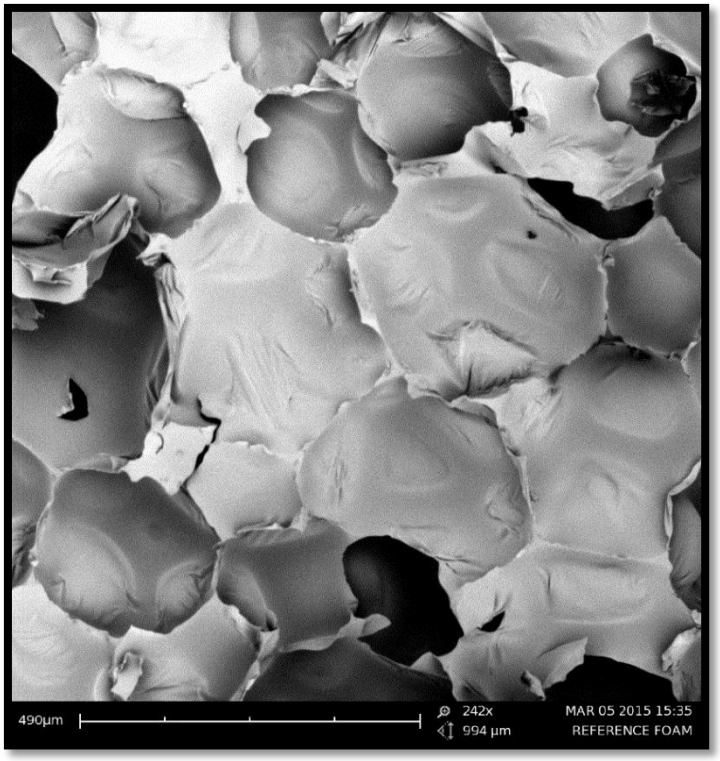

Figure 3.40: SEM image of the Reference Foam.

CHAPTER IV

CONCLUSION

Bio-based polyols were synthesized from the bio-based materials, β-caryophyllene and α-phellandrene, using 1-thioglycerol and 2-mercaptoethanol in varying molar equivalents by employing a photochemical thiol-ene coupling reaction. From these bio-based polyols, bio-based polyurethane foams were synthesized; their compositions were both 100% bio-based polyol and 50% bio-based polyol/50% Jeffol SG-360. A Reference Foam was prepared made from 100% Jeffol SG-360. This foam served as the industrial reference to which the properties of the novel polyurethane foams were compared in order to assess the viability of these novel polyurethane foams to serve the purpose of being used for applications such as thermal insulation of buildings, pipes, freezers and storage tanks. The novel polyurethane foams were superior to the Reference Foam in mechanical property. They were comparable to the Reference Foam in the areas of closed cell content % and density. They proved superior to the reference in the area of glass transition temperature and were found lesser than the reference in the area of thermal stability. Overall, it was concluded that the novel bio-based polyurethane foams

synthesized and studied in this research could serve as a viable option in industry for use as thermal insulation based on assessment of their properties.

REFERENCES

[1] X. Kong, G. Liu, H. Qi, J.M. Curtis, Prog. Org. Coat., 76 (2013) 1151-1160.

[2] L. Montero de Espinosa, M.A.R. Meier, Eur. Polym. J., 47 (2011) 837-852.

[3] G. Lligadas, J.C. Ronda, M. Galià, V. Cádiz, J. Polym. Sci. Part A: Polym. Chem., 51 (2013) 2111-2124.

[4] M. Ionescu, X. Wan, N. Bilić, Z. Petrović, J. Polym. Environ., 20 (2012) 647-658.

[5] V. Ribeiro da Silva, M.A. Mosiewicki, M.I. Yoshida, M. Coelho da Silva, P.M. Stefani, N.E. Marcovich, Polym. Test., 32 (2013) 438-445.

[6] Y.-h. Guo, J.-j. Guo, S.-c. Li, X. Li, G.-s. Wang, Z. Huang, Coll. Surf. A: Physicochem. Eng. Aspects, 427 (2013) 53-61.

[7] D.K. Chattopadhyay, D.C. Webster, Prog. Polym. Sci., 34 (2009) 1068-1133.

[8] S. Dworakowska, D. Bogdał, F. Zaccheria, N. Ravasio, Catal. Today, 223 (2014) 148-156.

[9] R.K. Gupta, M. Ionescu, D. Radojcic, X. Wan, Z.S. Petrovic, J. Polym. Environ., 22 (2014) 304-309.

[10] M.A.R. Meier, J.O. Metzger, U.S. Schubert, Chem. Soc. Rev., 36 (2007) 1788-1802.

[11] A. Guo, I. Javni, Z. Petrovic, J. Appl. Polym. Sci., 77 (2000) 467-473.

[12] M. Desroches, S. Caillol, V. Lapinte, R. Auvergne, B. Boutevin, Macromol., 44 (2011) 2489-2500.

[13] S. Tan, T. Abraham, D. Ference, C.W. Macosko, Polymer, 52 (2011) 2840-2846.

[14] E. Hablot, D. Zheng, M. Bouquey, L. Avérous, Macromol. Mater. Eng., 293 (2008) 922-929.

[15] R. Alfani, S. Iannace, L. Nicolais, J. Appl. Polym. Sci., 68 (1998) 739-745.

[16] J.L. Rivera-Armenta, T. Heinze, A.M. Mendoza-Martínez, Eur. Polym. J., 40 (2004) 2803-2812.

[17] K.L. Killops, L.M. Campos, C.J. Hawker, J. Am. Chem. Soc., 130 (2008) 5062-5064.

[18] S.P.S. Koo, M.M. Stamenović, R.A. Prasath, A.J. Inglis, F.E. Du Prez, C. Barner-Kowollik, W. Van Camp, T. Junkers, J. Polym. Sci. Part A: Polym. Chem., 48 (2010) 1699-1713.

[19] D.P. Nair, N.B. Cramer, T.F. Scott, C.N. Bowman, R. Shandas, Polymer, 51 (2010) 4383-4389.

[20] G. Lligadas, Macromol. Chem. Phys., 214 (2013) 415-422.

[21] J.F. Janes, I.M. Marr, N. Unwin, D.V. Banthorpe, A. Yusuf, Flavour Fragr. J., 8 (1993) 289-294.

[22] G.B. Bantchev, J.A. Kenar, G. Biresaw, M.G. Han, J. Agric. Food Chem., 57 (2009) 1282-1290.

[23] L.M. Campos, K.L. Killops, R. Sakai, J.M.J. Paulusse, D. Damiron, E. Drockenmuller, B.W. Messmore, C.J. Hawker, Macromol., 41 (2008) 7063-7070.

[24] J.P. Lafleur, R. Kwapiszewski, T.G. Jensen, Jörg P. Kutter, 16th International Conference on Miniaturized Systems for Chemistry and Life Sciences, Technical University of Denmark, Denmark, Warsaw University of Technology, Poland, 2012.

[25] C. Lluch, J.C. Ronda, M. Galià, G. Lligadas, V. Cádiz, Biomacromol., 11 (2010) 1646-1653.

[26] M. Bahr, R. Mulhaupt, Green Chem., 14 (2012) 483-489.

[27] K.P. Somani, S.S. Kansara, N.K. Patel, A.K. Rakshit, Int. J. Adhes. Adhes., 23 (2003) 269-275.

[28] M. Fleischer, H. Blattmann, R. Mulhaupt, Green Chem., 15 (2013) 934-942.

[29] Y. Gnanou, G. Hild, P. Rempp, Macromol., 17 (1984) 945-952.